Received: 19 December 2022 | Revised: 2 March 2023 | Accepted: 7 March 2023

DOI: 10.1002/ar.25212

SPECIAL ISSUE ARTICLE

The Anatomical Record WILEY

Virtual endocasts of *Clevosaurus brasiliensis* and the tuatara: Rhynchocephalian neuroanatomy and the oldest endocranial record for Lepidosauria

Lívia Roese-Miron[1] | **Marc Emyr Huw Jones**[2,3] | **José Darival Ferreira**[1] | **Annie Schmaltz Hsiou**[4]

[1]Programa de Pós-Graduação em Biodiversidade Animal, Universidade Federal de Santa Maria, Santa Maria, Brazil

[2]Science Group: Fossil Reptiles, Amphibians and Birds Section, Natural History Museum, London, UK

[3]Research Department of Cell and Developmental Biology, University College London, London, UK

[4]Departamento de Biologia, Faculdade de Filosofia, Ciências e Letras de Ribeirão Preto, Universidade de São Paulo, Ribeirão Preto, Brazil

Correspondence
Lívia Roese-Miron, Programa de Pós-Graduação em Biodiversidade Animal, Universidade Federal de Santa Maria, Avenida Roraima 1000, Santa Maria 97105-900, Brazil.
Email: livia.roem@hotmail.com

Funding information
Conselho Nacional de Desenvolvimento Científico e Tecnológico, Grant/Award Numbers: 130381/2020-9, 310948/2021-5; Fundação de Amparo à Pesquisa do Estado de São Paulo, Grant/Award Numbers: 2020/06819-5, 2019/14153-0; Australian Synchrotron; Coordenação de Aperfeiçoamento de Pessoal de Nível Superior, Grant/Award Numbers: 88887.714476/2022-00, 88887.819147/2023-00

Abstract

Understanding the origins of the vertebrate brain is fundamental for uncovering evolutionary patterns in neuroanatomy. Regarding extinct species, the anatomy of the brain and other soft tissues housed in endocranial spaces can be approximated by casts of these cavities (endocasts). The neuroanatomical knowledge of Rhynchocephalia, a reptilian clade exceptionally diverse in the early Mesozoic, is restricted to the brain of its only living relative, *Sphenodon punctatus*, and unknown for fossil species. Here, we describe the endocast and the reptilian encephalization quotient (REQ) of the Triassic rhynchocephalian *Clevosaurus brasiliensis* and compare it with an ontogenetic series of *S. punctatus*. To better understand the informative potential of endocasts in Rhynchocephalia, we also examine the brain-endocast relationship in *S. punctatus*. We found that the brain occupies 30% of its cavity, but the latter recovers the general shape and length of the brain. The REQ of *C. brasiliensis* (0.27) is much lower than *S. punctatus* (0.84–1.16), with the tuatara being close to the mean for non-avian reptiles. The endocast of *S. punctatus* is dorsoventrally flexed and becomes more elongated throughout ontogeny. The endocast of *C. brasiliensis* is mostly unflexed and tubular, possibly representing a more plesiomorphic anatomy in relation to *S. punctatus*. Given the small size of *C. brasiliensis*, the main differences may result from allometric and heterochronic phenomena, consistent with suggestions that *S. punctatus* shows peramorphic anatomy compared to Mesozoic rhynchocephalians. Our results highlight a previously undocumented anatomical diversity among rhynchocephalians and provide a framework for future neuroanatomical comparisons among lepidosaurs.

KEYWORDS

endocast, neuroanatomy, ontogeny, Rhynchocephalia, *Sphenodon punctatus*, Upper Triassic

1 | INTRODUCTION

The brain of extinct animals is rarely preserved, but aspects of its shape can sometimes be inferred using models of the brain cavity (Balanoff et al., 2016; Balanoff & Bever, 2017; Dozo et al., 2022). Such models (known as endocasts) can occur naturally (e.g., Bisconti et al., 2021; Triviño et al., 2018), be constructed artificially

with wax, latex, or similar materials (e.g., Dempster, 1935; Holloway, 2018; Paulina-Carabajal & Canale, 2010), or be generated digitally following nondestructive computed tomography (CT) and postprocessing of aligned slice data (e.g., Allemand et al., 2017, 2023; Balanoff et al., 2016; Perez-Martinez & Leal, 2021).

Endocasts can provide insights into anatomical and biological aspects of living and fossil taxa. For instance, they can be used to calculate measurements of relative brain size, such as the encephalization quotient (brain size in relation to body mass), which have been used to infer cognitive capacities in vertebrates (e.g., Hopson, 1977, 1979; Jerison, 1973, 1977; Lefebvre et al., 2004; Macrini et al., 2007; Marino, 2002). Endocast shape and the anatomy of the correspondent brain regions have also been correlated with phylogeny, sensory capacities, ecology, and behavior in both extant and extinct vertebrates (e.g., Allemand et al., 2017; Butler & Hodos, 1996; Carril et al., 2016; Corfield et al., 2012; Early et al., 2020; Lautenschlager et al., 2018; Macrini et al., 2007; Paulina-Carabajal, 2017; Sakai et al., 2011; Schade et al., 2022; Walsh & Knoll, 2011; Witmer et al., 2003). Besides the brain cavity, casts of other cranial spaces such as the endosseous labyrinth (inner ear), neurovascular canals, tympanic and paranasal pneumatic sinuses, and nasal cavities can provide similar information (e.g., Franco et al., 2021; Walsh et al., 2009; Witmer et al., 2003; Yi & Norell, 2015). Furthermore, endocasts of fossil species offer information about the evolutionary history of the neuroanatomy of different clades, which improves our understanding of the emergence of neuroanatomical disparity in vertebrates and the evolution of morphological patterns found in extant species (Balanoff & Bever, 2017; Dozo et al., 2022).

The shape and relative volume of endocranial casts can vary significantly during ontogeny, which can result from changes in skull shape, allometry, or distinct growth rates of the brain and the body. This variation is documented in taxa such as mammals (Ferreira et al., 2022; Macrini et al., 2007), crocodylians (Dufeau & Witmer, 2015; Dumont et al., 2020; Hu et al., 2021; Hurlburt et al., 2013; Jirák & Janáček, 2017; Lessner & Holliday, 2020; Watanabe et al., 2019), non-avian dinosaurs (Lautenschlager & Hübner, 2013), and birds (Hu et al., 2021; Watanabe et al., 2019). Most studies are concentrated on living species since obtaining multiple specimens of the same fossil species is usually not feasible (but see Dumont et al., 2020; Lautenschlager & Hübner, 2013, for examples with fossil dinosaurs and crocodylians, respectively). Studying the morphological changes that organisms go through throughout development can help delimitate the boundaries of intra and interspecific variation, as well as contribute to the refinement of diagnostic characters and improve the coding of character states in phylogenies (e.g., Abdala & Giannini, 2000; Kammerer et al., 2012). Thus, considering ontogenetic variation is fundamental in comparative studies (Watanabe et al., 2019).

Detailed cross-taxon comparisons of endocasts have helped illustrate the range of variation and identify patterns associated with size, phylogenetic affinity, and life history (e.g., Balanoff et al., 2013). The number of documented virtual endocasts has grown over the years, but sampling remains patchy. In the reptilian clade Lepidosauria (Squamata and Rhynchocephalia), knowledge of brain endocasts of extant species is restricted to squamates (Allemand, 2017; Allemand et al., 2017, 2023; Olori, 2010; Perez-Martinez & Leal, 2021; Scanferla, 2022; Segall et al., 2021), especially snakes (Allemand et al., 2017; Olori, 2010; Scanferla, 2022; Segall et al., 2021), which are highly specialized among lepidosaurs (Macrì et al., 2019). In relation to the endosseous labyrinth, a vast anatomical diversity is reported among living lepidosaurs (including the rhynchocephalian *Sphenodon punctatus*) (Bever et al., 2005; Olori, 2010; Palci et al., 2017; Walsh et al., 2009; Yi & Norell, 2015). Studies regarding endocasts of extinct species are scarcer. Both brain (Allemand, 2017; Camp, 1942) and endosseous labyrinth (Cuthbertson et al., 2015; Yi & Norell, 2019) endocasts have been described for some mosasauroids, as well as for the stem snake *Dinilysia patagonica* (Paulina-Carabajal et al., 2022; Scanferla, 2022; Triviño et al., 2018; Yi & Norell, 2015). However, no endocasts of fossil rhynchocephalians have yet been reported.

Rhynchocephalians were very common in the early Mesozoic, and may have surpassed the diversity of coeval squamates (e.g., DeMar Jr et al., 2022; Evans & Jones, 2010; Herrera-Flores et al., 2018; Hsiou et al., 2019; Whiteside, 1986; Wu, 1994). Fossil and molecular evidence suggests they originated close to the Permian–Triassic boundary (Burbrink et al., 2020; Gemmell et al., 2020; Jones et al., 2013; Simões et al., 2020), with the earliest fossils known from the Middle Triassic (Jones et al., 2013; Schoch & Sues, 2018). The clade possibly remained diverse until the Late Jurassic but became increasingly restricted to Gondwana by the Cretaceous (Anantharaman et al., 2022). Very few records are reported after the Cretaceous–Paleogene boundary, all coming from Gondwanan deposits (Anantharaman et al., 2022; Apesteguía et al., 2014; Jones, Tennyson, et al., 2009). More than 50 fossil rhynchocephalian species are known to date with a wide range of morphologies, habitats, and feeding ecologies (e.g., Evans & Jones, 2010; Jones, 2008; Meloro & Jones, 2012; Rauhut et al., 2012; Reynoso, 2000). Since these traits may be associated with differences in brain morphology, rhynchocephalians likely show variation in brain structure as other lepidosaurs do (see Hoops et al., 2017).

Many rhynchocephalian finds derive from South America, specifically Argentina (Apesteguía et al., 2012, 2014, 2021; Apesteguía & Carballido, 2014; Apesteguía & Jones, 2012; Apesteguía & Novas, 2003; Martínez et al., 2013) and Brazil (Bonaparte & Sues, 2006; Chambi-Trowell et al., 2021; Hsiou et al., 2019; Romo-de-Vivar et al., 2020). The cosmopolitan genus *Clevosaurus*, found from the Upper Triassic to the Lower Jurassic (and possibly Upper Jurassic) of different continents (Bonaparte & Sues, 2006; Fraser, 1988; Hsiou et al., 2019; Jones, 2006; Keeble et al., 2018; Klein et al., 2015; Säilä, 2005; Sues et al., 1994; Sues & Reisz, 1995; Wu, 1994), is represented in South America by two species (Bonaparte & Sues, 2006; Hsiou et al., 2019). *Clevosaurus brasiliensis* (Caturrita Formation, Paraná Basin), a Norian species of Southern Brazil, is one of the most well-known rhynchocephalians of the Upper Triassic (Arantes et al., 2009; Bonaparte & Sues, 2006; Hsiou et al., 2015). It is one of the smaller known species of the clade, with large orbits and a very short snout (Arantes et al., 2009; Bonaparte & Sues, 2006; Hsiou et al., 2015). The exceptional preservation of its skull remains makes it ideal for endocast analysis.

To interpret the context of the endocast of fossil rhynchocephalians, greater knowledge of the only extant species, *S. punctatus* (the tuatara), is required. The brain of *S. punctatus* is relatively well known (Abbie, 1934; Christensen, 1927; Dendy, 1909, 1911; Durward, 1930; Hindenach, 1931; Platel., 1989; Reiner & Northcutt, 2000; Starck, 1979), but its endocast remains undescribed, as does the spatial correspondence between its brain and endocast. *S. punctatus* is a medium-sized species endemic to New Zealand with high life expectancy, late sexual maturity (beyond 14 years long), cold physiology, and very slow reproduction, with egg-laying occurring once every 2–5 years (Castanet et al., 1988; Cree, 2014; Cree et al., 1991, 1992; Lamar et al., 2021; Scharf et al., 2015; Thompson & Daugherty, 1998). Historically, the tuatara was believed to be practically unchanged since the Mesozoic (Abbie, 1934; Edinger, 1951; Herrera-Flores et al., 2017; Hindenach, 1931; Reiner & Northcutt, 2000; Robb, 1977; Schwab & O'Connor, 2005), and regarded as a model for the ancestral amniote or reptile (e.g., Abbie, 1934; Edinger, 1951; Hindenach, 1931; Reiner & Northcutt, 2000; Robb, 1977). However, further studies on its anatomy and improved knowledge of the extensive fossil record of Rhynchocephalia have shown that this perception is unwarranted (e.g., Evans, 2003; Herrera-Flores et al., 2022; Jones, 2008; Jones & Cree, 2012; Jones, Curtis, et al., 2009; Jones, Tennyson, et al., 2009; Meloro & Jones, 2012; Vaux et al., 2018; Whiteside, 1986). Nevertheless, the species has a fundamental role for comparative studies among vertebrates as the sole end member of one of its lineages. Also, for many aspects of soft-tissue anatomy, it is the only available outgroup taxon for comparisons with Squamata (Jones, Curtis, et al., 2009).

Here, we describe the virtual endocast of *C. brasiliensis* (Upper Triassic, Norian) and compare its anatomy and encephalization quotient to an ontogenetic series of *S. punctatus*. We examine whether differences between the endocasts of *C. brasiliensis* and *S. punctatus* are related to size and allometry and provide a framework for future comparisons with other Rhynchocephalia. Additionally, we investigate this spatial and volumetric relationship in *S. punctatus*, given that the correspondence between endocast and brain can impact the informative potential of the former (Balanoff et al., 2013; Early et al., 2020; Watanabe et al., 2019). These are the first endocast descriptions for rhynchocephalians and the oldest record for lepidosaurs to date, thus providing an insight into early lepidosaur brain evolution.

2 | MATERIALS AND METHODS

2.1 | *Clevosaurus brasiliensis*

The species *C. brasiliensis* is found at the Linha São Luiz locality (53°30′23″W, 29°34′08″S) in the Faxinal do Soturno municipality, central region of the Rio Grande do Sul state, Brazil (Hsiou et al., 2015) (Figure 1). A 206Pb/238U date of 225.42 ± 0.37 Ma (Upper Triassic, Norian) was recovered for this site based on detrital zircon (Langer et al., 2018). It is characterized by massive, fine-grained sandstone beds and a typical *Riograndia* Assemblage Zone fauna, with small nonmammalian cynodonts, procolophonids, and lepidosaurs, as well as the dinosaur *Guaibasaurus candelariensis* (Bonaparte et al., 1999; Bonaparte et al., 2010; Soares et al., 2011). The *Riograndia* AZ represents the upper portion of the Candelária Sequence (Horn et al., 2014) or the basal portion of the Caturrita Formation (Andreis et al., 1980; Schultz et al., 2000; Zerfass et al., 2003) of the Paraná Basin, previously known as Santa Maria Sequence II (Zerfass et al., 2003). Our *C. brasiliensis* sample is comprised of one specimen (MCN PV 2852) (for institutional abbreviations, see Table 1) previously described by Hsiou et al. (2015). It is a well-preserved cranium, slightly compressed on the left side with disarticulated mandibles (Figure 1). Its braincase is preserved, being slightly displaced to the side. Most of its bones are externally damaged to a minor (supraoccipital, prootic, opisthotic) or major (basioccipital, exoccipital) degree (Hsiou et al., 2015), but its internal surface is mostly preserved and

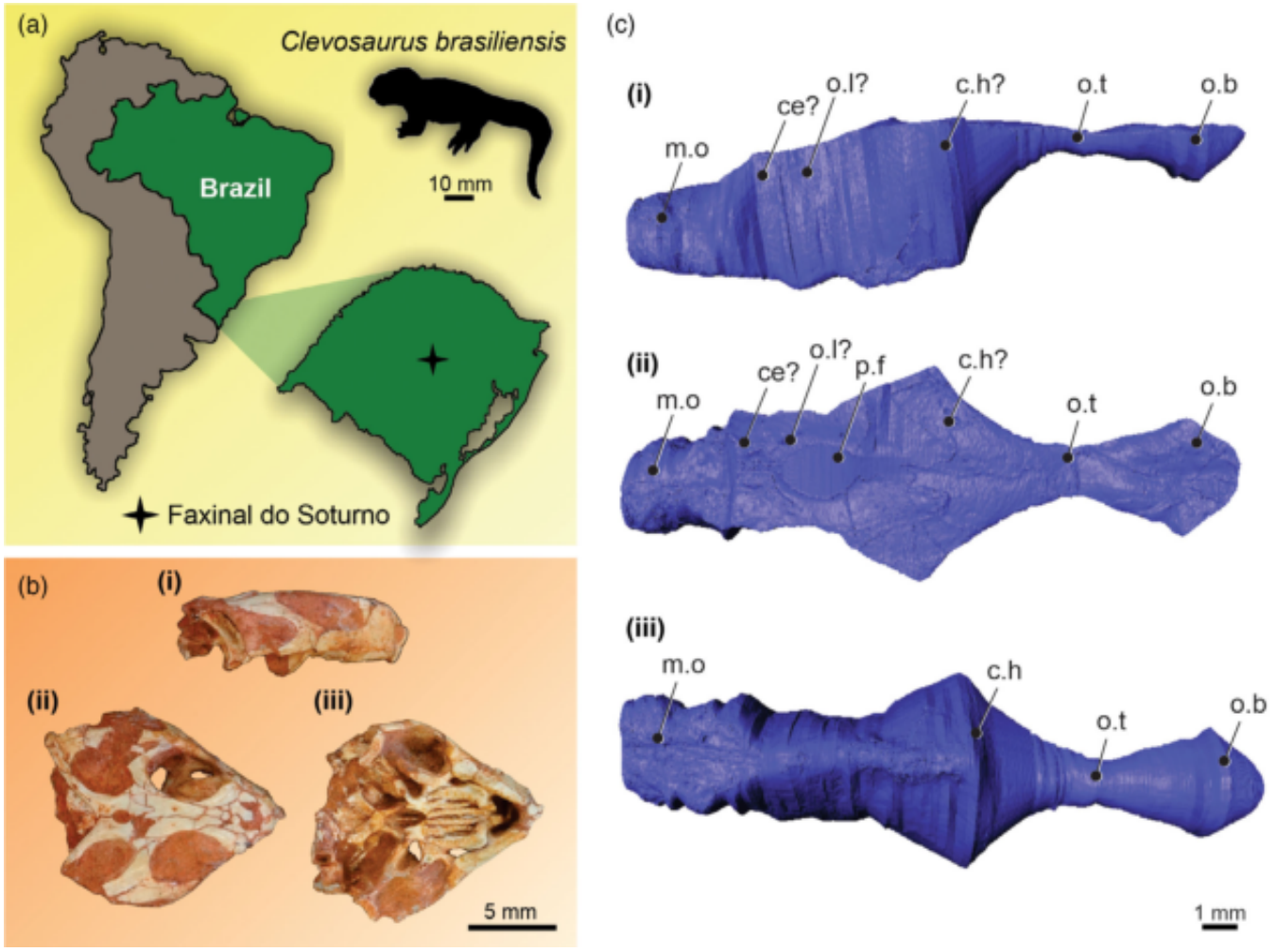

FIGURE 1 (a) Geographical occurrence and silhouette of *Clevosaurus brasiliensis* (scale bar: 10 mm). (b) Specimen MCN PV 2852 in lateral (i), dorsal (ii), and ventral (iii) views (scale bar: 5 mm). (c) Virtual endocast of the specimen in lateral (i), dorsal (ii), and ventral (iii) views (scale bar: 1 mm). ce, cerebellum; c.h, cerebral hemispheres; m.o, medulla oblongata; o.b, olfactory bulbs; o.l, optic lobes; o.t, olfactory tract; p.f, pineal foramen. A question mark is added after structures with uncertain position.

allows endocast reconstruction. The specimen can be confidently assigned as an adult due to developing a secondary bone "lip" in the maxilla and significant tooth wear (Hsiou et al., 2015).

2.2 | Sphenodon punctatus

The *S. punctatus* sample is composed of seven specimens in different ontogenetic stages: LDUCZ x1126 and CM 30660, two hatchlings (stage S1/S2); KCLZJ 001, a juvenile (T4); SU1, YPM HERR 009194 and SAMA 70524, three adults of similar size; and LDUCZ x0036, a huge adult, possibly indicating advanced age (Table 1). The ontogenetic stages of *S. punctatus* were classified based on skull length, degree of ossification of the skull, and differentiation of the lower dentition (when available), following existing documentation on its ontogeny (Apesteguía & Carballido, 2014; Dendy, 1899; Harrison, 1901; Rieppel, 1992; Robinson, 1976). Except for one confirmed female with eggs inside (SU1), sex data were not available.

2.3 | Computed tomography and endocast generation

The *S. punctatus* specimens were scanned prior to this study, and the CT specifications of each scanning are available in the supplementary material (Table S1). The CT scan files of YPM HERR 009194 and CM 30660 were obtained from the online repository digimorph.org (Maisano, 2001a, 2001b). One of the specimens of *S. punctatus* (SAMA 70524), preserved in an ethanol solution, had undergone a process called diffusible iodine-based contrast-enhanced CT: its head had already been

TABLE 1 Specimens included in this study with their repositories (institutions) and ontogenetic stage

Species	Specimen	Institution	Ontogenetic stage
Clevosaurus brasiliensis	MCN PV 2852	Museu de Ciências Naturais, Secretaria do Meio Ambiente e Infraestrutura do Estado do Rio Grande do Sul (Porto Alegre, Brazil)	Adult
Sphenodon punctatus	LDUCZ x1126	Grant Museum of Zoology, University College London (London, United Kingdom)	Hatchling (S1/S2)
S. punctatus	CM 30660	Carnegie Museum of Natural History (Pennsylvania, United States)	Hatchling (S1/S2)
S. punctatus	KCLZJ 001	The Museum of Life Sciences, King's College London (London, United Kingdom)	Juvenile (T4)
S. punctatus	SU1	Marc Jones personal collection	Adult
S. punctatus	YPM HERR 009194	Yale Peabody Museum (Connecticut, United States)	Adult
S. punctatus	SAMA 70524	South Australian Museum (Adelaide, Australia)	Adult
S. punctatus	LDUCZ x0036	Grant Museum of Zoology, University College London (London, United Kingdom)	Big (old?) adult

fixed with formalin and was stained in 7.5% I2KI for 24 days prior scanning. It significantly improves the visibility of different tissues (Gignac et al., 2016; Gignac & Kley, 2018), allowing brain segmentation. The brain cavity, endosseous labyrinth, and initial trunks of the cranial nerves were reconstructed through manual segmentation with a digitizing table in Avizo 3D. In this method, the cavities are identified and filled in each slice (bidimensional parallel images that compose the CT scan), with the subsequent generation of a 3D surface model. All 3D surfaces were exported as .ply files, and they are available at the online repository MorphoMuseuM (Roese-Miron et al., 2023) and as 3D PDF files in the Supplementary Material.

In *C. brasiliensis*, there is no ossified skeleton surrounding the ventrolateral surface of the brain cavity between the olfactory bulbs and the anterior limit of the sella turcica of the parabasisphenoid, which meant that these surfaces had to be approximated. Anteriorly to the parabasisphenoid, the ventral extent of the endocast was delimited by the cultriform process, which projects anteriorly quite extensively. Despite the actual endocast likely not contacting the cultriform process, it is the only definitive osteological correlate that can be used, since the endocast cannot surpass it ventrally. Therefore, it represents a "maximum limit" of the ventral surface of the endocast. The height of the olfactory tract was determined using *Sphenodon* as a guide. Finally, an approximately straight line was drawn between the approximate posterior end of the olfactory tract ventral surface until the anterior end of the cultriforme process. Since these surfaces cannot be precisely recovered, endocast height measurements (and to some extent its volume) should be considered conservative approximations.

2.4 | Descriptions and quantitative analyses

The anatomy of all models was described comparatively. To contribute to the descriptions and investigate allometric patterns, a series of measurements was obtained using Avizo 3D (supplementary material, Figure S1) (cf. Allemand et al., 2017; Lautenschlager & Hübner, 2013; Walsh et al., 2009). We took 13 linear measurements (plus the volume) from the brain cavity and brain models and eight measurements exclusively from the brain. We also measured the angle of the pontine (angle between hindbrain and midbrain) and cephalic (angle between midbrain and forebrain) flexures. The flexures were calculated three times for each specimen, and a mean of these values was used (cf. Cooper & Purvis, 2009). Given that the endocast and brain measurements are not necessarily equivalent (even if they use the closest possible reference points), different abbreviations were used to avoid merging endocast and brain data. Additionally, we took four measurements from the skull and four from the endosseous labyrinth, using the mean of the left and right sides.

To evaluate the allometric growth of the endocast throughout *S. punctatus* ontogeny, we generated the following bivariate linear regressions: (a) endocast measurements against skull measurements; (b) endocast linear measurements against endocast volume (EV); and (c) endocast linear measurements against endocast total length. All the

axes were $\log_{10}$-transformed. The statistical information (slope, intercept, and r^2) is shown in the corresponding figures. Posteriorly, the same regressions were performed with the inclusion of *C. brasiliensis*. Significance was defined when $p \leq .05$. We also calculated and compared simple proportions between these measurements (a–c). All the regressions were performed in the software PAST (Hammer et al., 2001).

2.5 | Reptilian encephalization quotient

We calculated the reptilian encephalization quotient (REQ) for *S. punctatus* and *C. brasiliensis* using the equation in Hurlburt (1996):

$$\mathrm{REQ} = \mathrm{MBr}/\left(0.0155 \times \mathrm{MBd}^{0.55}\right)$$

In which MBR is brain mass (g) and Mbd is body mass (g). Body mass information was unavailable for the specimens, so it had to be estimated. Allometric functions are one of the most common ways to estimate body mass in living and fossil species since it needs few measurements (Köhler et al., 2008). Thus, we used a model to predict body mass based on skull width using a database of 29 specimens of *S. punctatus* with body masses between 200 and 840 g (all data are available in the Supplementary Material). This model was used to predict the masses of all specimens in our sample, including *C. brasiliensis*, given that there is evidence that the body mass of extinct species can be estimated based on extant ones if their form and morphology is similar (Christiansen & Fariña, 2004; Farlow et al., 2005; Gingerich, 1990; Hurlburt, 1999). All analyses were performed using R software with the packages "tidyverse" and "ggfortify" installed.

To estimate the brain mass, two proportions of the EV were used: the value found by the present study for *S. punctatus* (i.e., 0.3) and 0.5, which is the value classically assumed for non-avian reptiles, including *S. punctatus* (e.g., Balanoff & Bever, 2017; Hopson, 1979; Jerison, 1973). The ontogenetic variation of the volumetric correspondence between the brain and brain cavity was not evaluated here. Still, likely, the value found here (based on one adult specimen) does not represent all ontogenetic stages. Therefore, 0.5 may be a more ontogenetically inclusive estimation for this calculation (based on the intermediate value found in an ontogenetic series of *Alligator mississippiensis*; Hurlburt et al., 2013). Since the specific density of the brain is approximately 1 g/cm (Jerison, 1973), the volume of the endocast was converted to cubic centimeters and multiplied by the two proportions mentioned above to obtain the brain mass. Given that the brain and body masses are estimations, the resulting REQ values are likely approximations.

3 | RESULTS

3.1 | *C. brasiliensis* endocast

The basicranium of *C. brasiliensis* is slightly displaced to the right in relation to the skull, but the general endocast shape is recovered (Figure 1). The endocast has a subtle angulation laterally, with an almost straight dorsal surface and a more ventral hindbrain. The olfactory tract, covered dorsally by the frontal bone, narrows laterally in its median portion and expands anteriorly toward the olfactory bulbs. The anterior end of the olfactory bulbs was delimitated based on the division between the frontal and the nasal bones. The separation between the posterior end of the olfactory tract and the cerebral hemispheres is not visible. Still, it seems to occur (based on endocast width) slightly anteriorly to the frontoparietal suture (of which the impression is visible on the dorsal surface of the endocast). The cerebral hemispheres, optic lobes, and cerebellum are not distinguishable from one another; the surface of their region is diamond-shaped in dorsal view, roofed dorsally by the frontal and parietal bones. Posteriorly, at the level of the optic lobes and cerebellum, the endocast narrows laterally, and its lateral faces become almost parallel until the beginning of the medulla oblongata. In the dorsal face, an impression of a large oval pineal foramen is left by the contact of the parietal.

From the approximate posterior end of the olfactory tract, the ventral surface of the endocast projects posteroventrally until the cultriforme process of the parabasisphenoid, nearly at the vertical level of the frontoparietal suture. From the anterior limit of the cultriforme process, the ventral surface of the endocast directs itself almost horizontally until its posterior end. There is a subtle ventral recess or indentation in the lateral view of the endocast between the cultriform process and the pituitary fossa of the parabasisphenoid. Posteriorly to the pituitary fossa, the contact of the ventral surface of the endocast with the basicranium broadens until the posterior end of the model. The lateral surfaces of the medulla oblongata are practically parallel, and its ventral surface is flat (but this shape may be exaggerated by the taphonomy of the basicranium). The medulla oblongata region presents a lateral constriction that would accommodate the inner ear, being more exaggerated in its dorsalmost portion where the *common crus* would be located. The cranial nerves were not identifiable, as well as the endosseous labyrinth, due to the poor preservation of the otic capsule. Because of the lack of semicircular canals, the

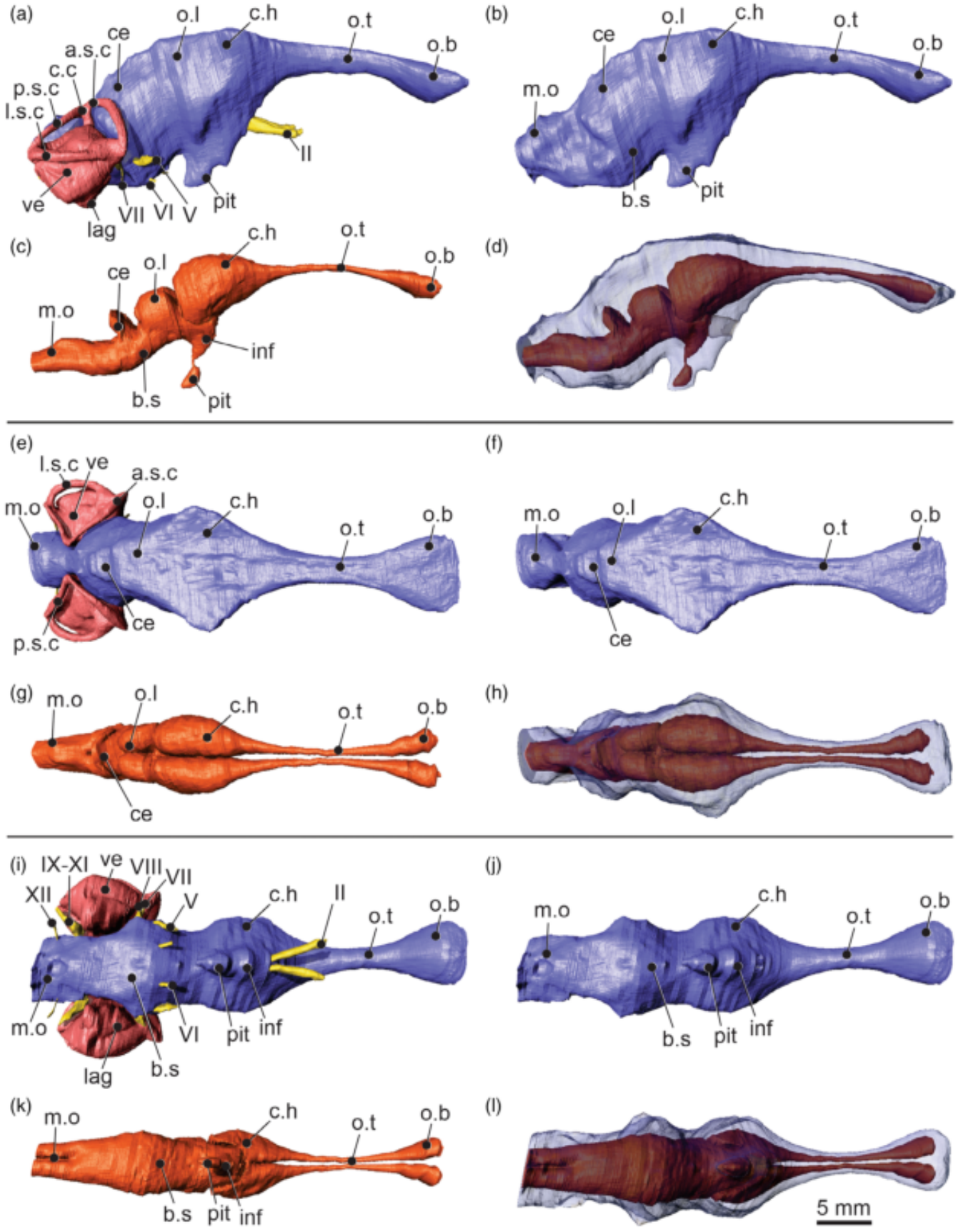

FIGURE 2 Legend on next page.

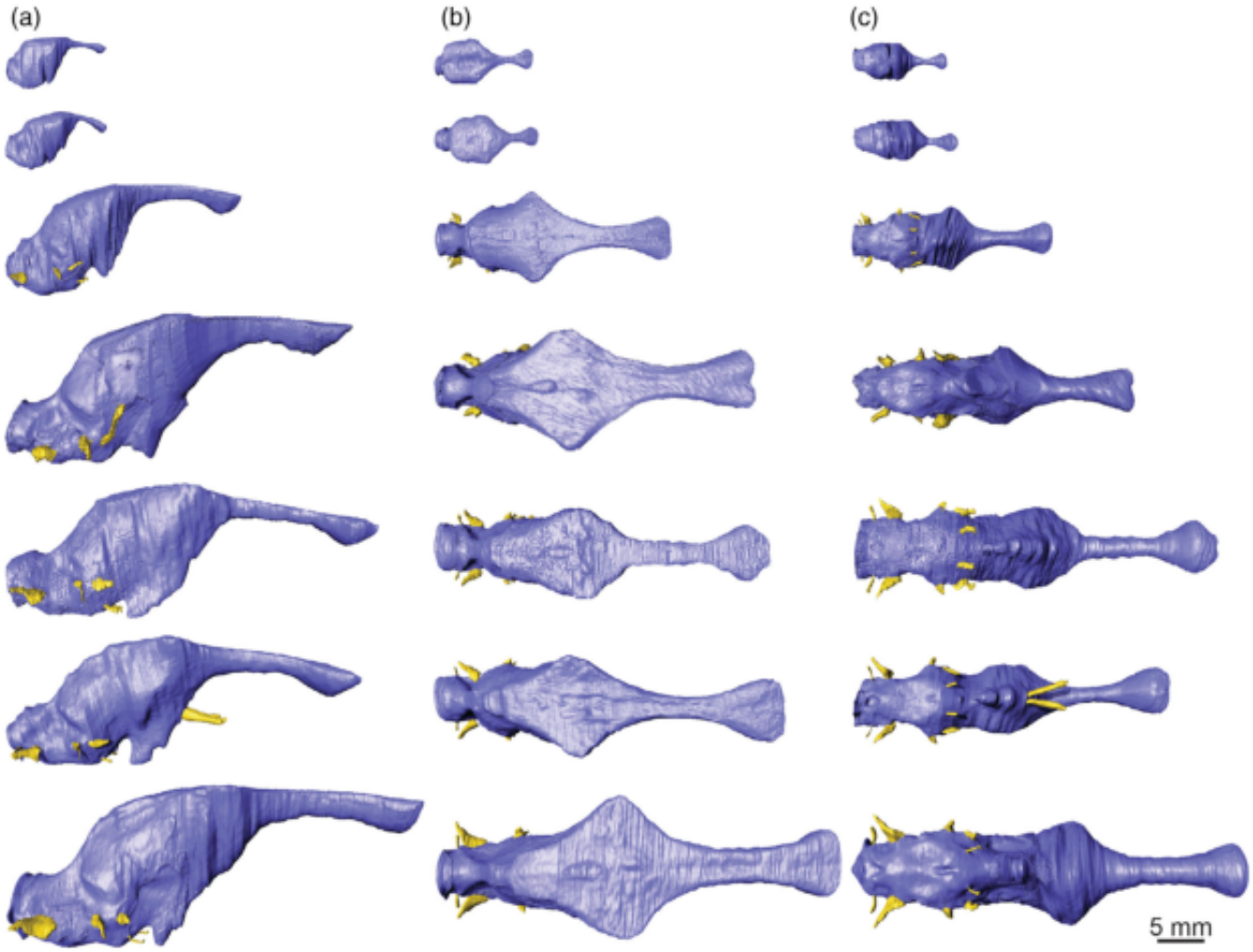

FIGURE 3 Virtual endocasts and cranial nerves of *Sphenodon punctatus* throughout ontogeny in lateral (a), dorsal (b), and ventral (c) views. Specimens from top to bottom of each column: LDUCZ x1126 (hatchling, stage S); CM 30660 (hatchling, stage S); KCLZJ 001 (juvenile, stage T); SU1 (adult); YPM HERR 009194 (adult); SAMA 70524 (adult); LDUCZ x036 (adult). Scale bar: 5 mm.

endocast was aligned maintaining the dorsal surface of the region of the cerebral hemispheres horizontal (Figure 1), but this is not meant to represent the active posture of the species necessarily.

3.2 | *S. punctatus* endocast and ontogenetic variation

The endocast of the adult *S. punctatus* (Figure 2) is similar in general shape to *C. brasiliensis*, but some characteristics distinguish them. In the tuatara, it is dorsoventrally curved in lateral view, with the flexures becoming less pronounced during ontogeny (Figure 3), following the "uncoiling" of the skull. However, even in the bigger specimen, the angles of the pontine and cephalic flexures are less obtuse than in *C. brasiliensis* (respectively, 142.42° and 138.28° for *S. punctatus*, and 158.02° and 158.05° for *C. brasiliensis*) (Figure 7; Table 2).

The olfactory tract is narrow, ending anteriorly in expanded olfactory bulbs. This narrow portion is very short in the juveniles, as in *C. brasiliensis*, but it is more

FIGURE 2 Virtual endocasts of *Sphenodon punctatus* (SAMA 70524) in lateral (a–d), dorsal (e–h), and ventral (i–l) views. Structures by color: brain (orange), cranial nerves (yellow), endocast (blue), and endosseous labyrinth (pink). Overlap of the endocast (transparency) and brain in d, h, and l. a.s.c, anterior semicircular canal; b.s, brain stem; c.c, *common crus*; ce, cerebellum; c.h, cerebral hemispheres; inf, infundibulum; lag, lagena, l.s.c, lateral semicircular canal; m.o, medulla oblongata; o.b, olfactory bulbs; o.l, optic lobes; o.t, olfactory tract; pit, pituitary gland; p.s.c, posterior semicircular canal; ve, vestibule; II, V-XII, initial trunks of the cranial nerves. Scale bar: 5 mm.

TABLE 2 Measurements of the endocast, endosseous labyrinth, and skull of *Sphenodon punctatus* and *Clevosaurus brasiliensis*

Skull measurement	LDUCZ x1126	CM 30660	KCLZJ 001	SU1	YPM HERR 009194	SAMA 70524	LDUCZ x0036	MCN PV 2852
SL1 (mm)	12.23	14.00	34.43	54.37	56.30	57.69	73.93	20.13
SL2 (mm)	13.62	14.75	33.47	49.84	51.81	52.21	66.10	22.44
SW (mm)	9.16	10.63	25.43	43.41	44.23	42.65	53.39	20.76
BW (mm)	7.65	8.21	15.48	30.67	31.02	27.98	33.93	14.52
Endocast measurement	**LDUCZ x1126**	**CM 30660**	**KCLZJ 001**	**SU1**	**YPM HERR 009194**	**SAMA 70524**	**LDUCZ x0036**	**MCN PV 2852**
EV (mm^3)	89.84	108.50	521.41	1,185.22	1,325.08	1,350.37	2,221.94	124.88
EL (mm)	11.30	12.05	25.83	35.70	41.02	40.13	46.80	18.50
CHW (mm)	4.71	5.00	8.66	11.28	9.62	9.71	14.53	5.98
OTL (mm)	4.65	4.46	10.81	12.46	16.22	16.57	18.65	7.20
OBH (mm)	0.98	1.17	2.15	3.62	2.82	3.15	3.79	1.39
PH (mm)	5.08	5.44	9.53	12.71	12.75	12.91	15.91	4.11
BSMW (mm)	4.31	4.16	6.64	6.61	8.01	8.60	8.73	3.21
HML (mm)	3.76	3.99	8.70	11.36	11.97	13.09	14.01	5.83
BSAW (mm)	4.05	4.06	6.12	6.22	6.40	6.53	7.78	3.08
IEW (mm)	1.37	1.97	2.45	2.21	2.72	2.18	2.44	1.36
PPH (mm)	0.37	0.52	1.61	2.50	2.18	3.27	2.76	—
PW (mm)	0.71	0.45	1.23	2.07	0.97	1.24	2.68	—
FP (°)	124.94	126.82	136.88	139.37	144.78	145.35	142.42	158.02
FC (°)	122.37	117.36	125.15	133.43	135.33	131.67	138.28	158.05
Inner ear measurement	**—**	**—**	**KCLZJ 001**	**SU1**	**YPM HERR 009194**	**SAMA 70524**	**LDUCZ x0036**	**—**
LL (mm)	—	—	1.66	2.13	2.02	2.43	3.03	—
SAL (mm)	—	—	4.03	6.81	7.1	6.92	7.74	—
SLL (mm)	—	—	5.07	5.96	5.93	5.89	7.69	—
SPL (mm)	—	—	3.14	4.86	4.37	4.64	6.28	—

Abbreviations: BSAW, brain stem anterior width; BSMW, brain stem maximum width; BW, basicranium width; CHW, cerebral hemispheres width; EL, endocast length; EV, endocast volume; FC, cephalic flexure; FP, pontine flexure; HML, hindbrain + midbrain length; IEW, inner ear region width; LL, lagena length; OBH, olfactory bulbs height; OTL, olfactory tract length; PH, posterior height; PPH, pituitary posterior height; PW, pituitary bulb width; SAL, anterior semicircular canal length; SL1, skull length (premaxilla – posterior limit of the quadrate); SL2, skull length (premaxilla – posterior limit of the basicranium); SLL, anterior semicircular canal length; SPL, lateral semicircular canal length; SW, skull width.

elongated in adults (Figure 3). The ventrolateral surface from the olfactory bulb to the beginning of the contact with the basicranium is also not enclosed by bone. Still, its delimitation is much more precise due to the difference in density of the tissues in the living species. From the posterior end of the olfactory tract to the pituitary prominence, the ventral surface is approximately straight and becomes less vertical during ontogeny (Figure 3). The posterior region of the pituitary prominence is separated from the hindbrain by the cast of the mesencephalic flexure, which becomes more pronounced during ontogeny. The ventral surface of the hindbrain is rounded and concave in the younger specimens, with a recess developing in its anterior portion in the adults. Such a difference reflects changes to the shape of the enclosing basicranium.

The boundaries between the cerebral hemispheres, optic lobes, and cerebellum are not visible in juveniles and adults (Figure 2). The impression of a drop-shaped pineal foramen is visible in the dorsal surface. The shape of this region shows clear ontogenetic differences in the dorsal view: in juveniles, it is trapezoidal with a slight medial constriction, whereas, in adults, it is diamond-shaped (Figure 3). The medulla oblongata presents a lateral constriction in its dorsal portion that accommodates the *common crus* of the inner ear. In juveniles, this

constriction is subtler, as seen in *C. brasiliensis*, being way more accentuated in adults. In ventral view, the region at the vertical height of the cerebral hemispheres is laterally expanded. This is followed posteriorly by a lateral constriction at the approximate height of the optic lobes. This constriction is very pronounced in adults but barely present in juveniles. Posterior to this, the endocast expands laterally again approximately at the vertical height of the cerebellum region. The endocast narrows when reaching the medulla oblongata, with its lateral surfaces becoming approximately parallel.

3.3 | *S. punctatus* cranial nerves and endosseous labyrinth

The initial trunks of the cranial nerves XII through V were identifiable in the five bigger specimens (Figure 3) and nerve II in specimen SAMA 70524 (Figure 2). The nerves XII-V departure ventrolaterally from the hindbrain, approximately from the same horizontal plane (except the more ventral nerve VI), and their position is consistent with previous descriptions and illustrations for the species (Dendy, 1909; Wyeth, 1920). The hypoglossal nerve (XII) leaves from the posteriormost portion of the medulla oblongata. The accessory (XI), vagus (X), and glossopharyngeal (IX) nerves are accommodated adjacent to a recess in the posteromedial surface of the inner ear. There is a marked ventrolateral projection in the hindbrain, approximately at the level of the cerebellum, from where the facial (VII) and vestibulocochlear (VIII) nerves depart, sharing the same root (Dendy, 1909). The trigeminal nerve (V) is located slightly anterior and dorsal to them. The narrow abducent nerve (VI) departures from the same vertical plane of V, but more ventrally. Anteriorly to the pituitary gland, the thick optic nerve (II) directs anteroventrally until it reaches the eyes.

The endosseous labyrinth was segmented in all but the two hatchlings specimens due to their lack of ossification of the otic capsule. The models of the other five specimens are very similar, mainly varying in size, so they are described conjunctly based on the specimen SAMA 70524 (Figure 4). The following description is consistent with previous accounts on the anatomy of the inner ear of *S. punctatus* (e.g., Gans & Wever, 1976; Wyeth, 1920). The vestibule (saccule and the utricle) is large, almost ellipsoid in the dorsal view, and losangular in the lateral view. In its posterolateral face, it is possible to see the impression left by the oval foramen. The three semicircular canals are somewhat narrow and easily distinguishable. The lateral canal is the longest, forming a wide arch practically horizontal to the plain of the head. Between it and the anterior canal, an expansion corresponds to the

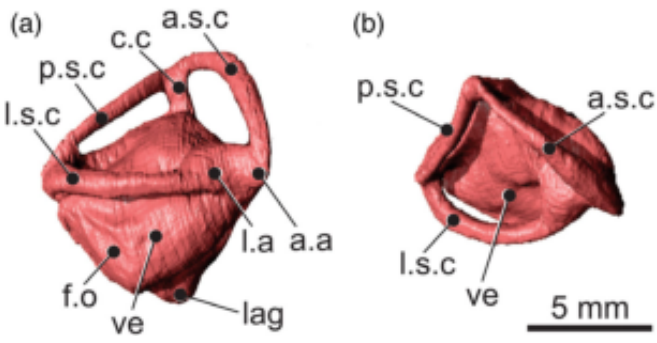

FIGURE 4 Endosseous labyrinth of *Sphenodon punctatus* (SAMA 70524). Right side, lateral (a) and dorsal (b) views. a.a, anterior ampulla; a.s.c, anterior semicircular canal; c.c, *common crus*; f.o, oval foramen; l.a, lateral ampulla; lag, lagena, l.s.c, lateral semicircular canal; p.s.c, posterior semicircular canal; ve, vestibule. Scale bar: 5 mm.

lateral and anterior ampullae. The anterior canal also forms an arch, directing dorsomedially as it advances posteriorly. It forms an angle of approximately 45° (in dorsal view) with the sagittal plain of the head. The anterior canal is united with the posterior canal by the *common crus*, a short vertical canal that directs ventrally to the vestibule. The posterior semicircular canal is the shortest; it is almost straight, descending posteriov until it reaches the posterior extremity of the lateral canal. The lagena (or cochlear duct) is relatively short, leaving the saccule and directing itself ventromedially. This type of short and almost conical cochlear duct, also seen in some squamates (Olori, 2010; Palci et al., 2017; Yi & Norell, 2015), has been related to low-frequency hearing (Manley, 1972; Walsh et al., 2009). Indeed, previous tests showed that *S. punctatus* can hear sounds below 2,000 Hz received through air and substrate (Gans & Wever, 1976), despite its lack of a tympanic membrane (Evans, 2016).

3.4 | Brain and endocast comparison in adult *S. punctatus*

The endocast reflects the general shape of the brain of *S. punctatus* (Figure 2), but there are issues to be aware of. The specimen SAMA 70524 was preserved in an ethanol solution for an unknown but extended period before scanning, which could lead to a certain degree of shrinkage in the brain. However, the presence of surrounding connective tissues can provide structural support and shape integrity (Vickerton et al., 2013), and brain shape does not seem to have been affected (see Dendy, 1911). We found that the brain volume corresponds to only 0.3 (i.e., 30%) of the volume of the brain cavity, a value that

TABLE 3 Measurements of the endocast and brain of *Sphenodon punctatus* (SAMA 70524), and proportion between brain and endocast measurements

Endocast measurements		Brain measurements		Brain/endocast
EV	1,350.37 mm^3	BV	404.96 mm^3	0.300
EL	40.13 mm	BL	38.85 mm	0.968
CHW	9.71 mm	B.CHW	6.75 mm	0.695
OTL	16.57 mm	B.OTL	15.98 mm	0.964
OBH	3.15 mm	B.OBH	2.08 mm	0.660
PH	12.91 mm	B.PH	5.96 mm	0.462
BSMW	8.60 mm	B.BSMW	5.50 mm	0.640
HML	13.09 mm	B.HML	14.19 mm	1.084
BSAW	6.53 mm	B.BSAW	4.40 mm	0.674
IEW	2.18 mm	B.IEW	2.18 mm	1.000
PPH	3.27 mm	B.PPH	4.98 mm	1.523
PGW	1.24 mm	B.PGW	0.88 mm	0.710
—		B.CHL	8.16 mm	—
—		B.CBDW	4.51 mm	—
—		B.OLL	3.93 mm	—
—		B.OLH	5.74 mm	—
—		B.OLDW	5.37 mm	—
—		B.PIH	7.68 mm	—
—		B.PW	3.28 mm	—

Abbreviations: B. BSAW, brain stem anterior width (brain); B.BSMW, brain stem maximum width (brain); B.CBDW, cerebellum dorsal width (brain); B.CHL, cerebral hemispheres length (brain); B.CHW, cerebral hemispheres width (brain); B.HML, hindbrain + midbrain length (brain); B.IEW, inner ear region width (brain); B.OBH, olfactory bulbs height (brain); B.OLDW, optic lobes dorsal width (brain); B.OLH, optic lobes height (brain); B.OLL, optic lobes length (brain); B.OTL, olfactory tract length (brain); B.PGW, pituitary gland width (brain); B.PH, posterior height (brain); B.PIH, pituitary + infundibulum height (brain); B.PPH, pituitary posterior height (brain); B.PW, pituitary bulb (or infundibulum) width (brain); BL, brain length; BSAW, brain stem anterior width (endocast); BSMW, brain stem maximum width (endocast); BV, brain volume; CHW, cerebral hemispheres width (endocast); EL, endocast length; EV, endocast volume; HML, hindbrain + midbrain length (endocast); IEW, inner ear region width (endocast); OBH, olfactory bulbs height (endocast); OTL, olfactory tract length (endocast); PGW, pituitary gland width (endocast); PH, posterior height (endocast); PPH, pituitary posterior height (endocast).

is considerably lower than the previously used brain-to-endocast correspondence (BEC) of 0.5 for the species (e.g., Balanoff & Bever, 2017).

The lateral expansions responsible for the endocast diamond shape in the dorsal view are not present in the brain. The cerebral hemispheres, optic lobes, and cerebellum are markedly separated in the brain, and the olfactory tract and bulbs are narrower and bipartite. Continuous to this bipartition, a deep median interhemispheric fissure medially divides the cerebral hemispheres and optic lobes. The cerebral hemispheres are oval in dorsal view; their posteroventral limit is marked by a suture that separates them from the infundibulum. A deep fissure separates the cerebral hemispheres from the optic lobes. The latter are also oval in dorsal view but smaller. The optic lobes are separated from the slightly concave cerebellum by a wide gap, and ventrally, they end at the brain stem without clear separation. In the ventral view, the slight lateral expansions of the forebrain and hindbrain are much less pronounced than in the endocast. The medulla oblongata narrows posteriorly; in its ventral surface, there is a pronounced medial fissure, where the inferior spinal artery is possibly accommodated (Dendy, 1909). Despite these disparities, some dimensions are surprisingly similar between the endocast and the brain. The endocast length (EL) and brain length (BL), endocast olfactory tract length (OTL) and brain olfactory tract length (B.OTL), endocast hindbrain + midbrain length (HML) and brain hindbrain + midbrain length (B.HML) and endocast inner ear region width (IEW) and brain inner ear region width (B.IEW) present a correspondence of 90–100%, with the remaining dimensions showing a correspondence between 70 and 50% (for complete results, see Table 3). Also, the endocast is very close to the brain in the ventral surface of the pituitary and the ventral surface of the olfactory tract.

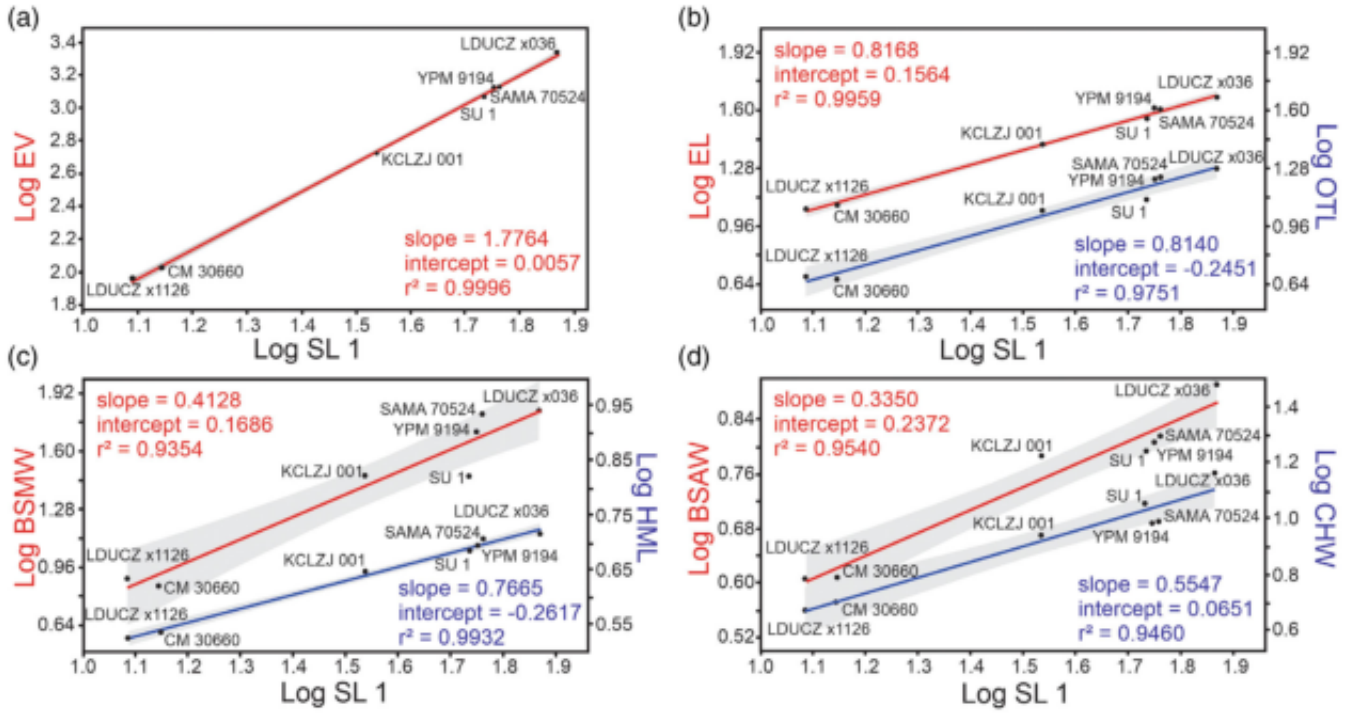

FIGURE 5 Linear regressions of skull length and endocast dimensions of *Sphenodon punctatus*. Skull length (premaxilla – quadrate) plotted against (a) endocast volume (EV); (b) endocast length (EL), and olfactory tract length (OTL); (c) brain stem maximum width (BSMW) and hindbrain + midbrain length (HML); and (d) brain stem anterior width (BSAW) and cerebral hemispheres width (CHW). All axes are log-transformed. Two regressions are represented in each plot in b–d; the axis, graph line, and regression statistics (slope, intercept, r^2) are identified with the same color (red and blue) in each plot. Confidence intervals are indicated in gray, and all p-values ≤.05.

TABLE 4 Endocast measurements in proportion to skull and endocast length. *Sphenodon punctatus* specimens are shown from smaller to bigger, and *Clevosaurus brasiliensis* is shown in the last column. EV/SL1 was calculated with log-transformed values

	LDUCZ x1126	CM 30660	KCLZJ 001	SU1	YPM 9194	SAMA 70524	LDUCZ x036	MCN PV 2852
EV/SL1	1.8	1.78	1.77	1.77	1.78	1.78	1.79	1.61
EL/SL1	0.92	0.86	0.75	0.66	0.73	0.7	0.63	0.92
OTL/SL1	0.38	0.32	0.31	0.23	0.29	0.29	0.25	0.36
HML/SL1	0.31	0.29	0.25	0.21	0.21	0.23	0.19	0.59
CHW/SL1	0.39	0.36	0.25	0.21	0.17	0.17	0.2	0.3
BSAW/SL1	0.33	0.29	0.18	0.11	0.11	0.11	0.11	0.15
BSMW/SL1	0.35	0.3	0.19	0.12	0.14	0.15	0.12	0.16
CHW/EL	0.42	0.41	0.34	0.32	0.23	0.24	0.31	0.32
BSAW/EL	0.36	0.34	0.24	0.17	0.16	0.16	0.17	0.17
BSMW/EL	0.38	0.35	0.26	0.19	0.2	0.21	0.19	0.17
IEW/EL	0.12	0.16	0.09	0.06	0.07	0.05	0.05	0.07

Abbreviations: BSAW, brain stem anterior width; BSMW, brain stem maximum width; CHW, cerebral hemispheres width; EL, endocast length; EV, endocast volume; HML, hindbrain + midbrain length; IEW, inner ear region width; OTL, olfactory tract length; SL1, skull length (premaxilla – quadrate).

3.5 | Allometric relationships

Throughout *S. punctatus* ontogeny, all dimensions of the endocast show a positive relationship with the dimensions of the skull (Figure 5). The relationship between EV and skull length is isometric, whereas the linear measurements mainly change allometrically, with the endocast/skull proportions decreasing through ontogeny (Table 4). The endocast measurements also show a positive allometric relationship with EL (supplementary

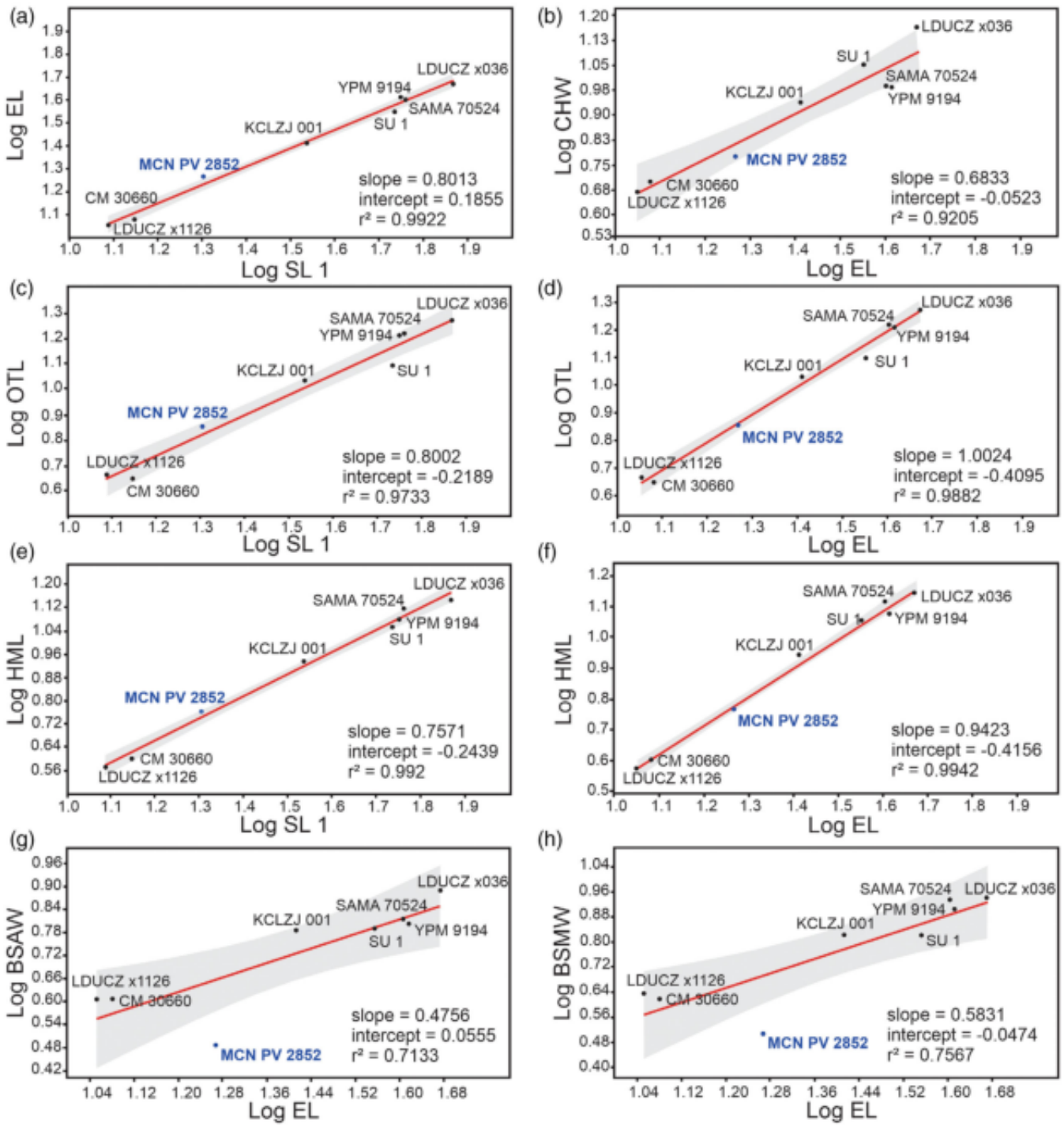

FIGURE 6 Linear regressions of skull and endocast measurements of *Sphenodon punctatus* and *Clevosaurus brasiliensis*. Skull length (premaxilla – quadrate) (SL1) plotted against (a) endocast length (EL), (c) olfactory tract length (OTL), and (e) hindbrain + midbrain length (HML). Endocast length (EL) plotted against (b) cerebral hemispheres width (CHW), (d) olfactory tract length (OTL), (f) hindbrain + midbrain length (HML), (g) brain stem anterior width (BSAW), and (h) brain stem maximum width (BSMW). *Clevosaurus brasiliensis* (MCN PV 2852) highlighted in blue. All axes are log-transformed. Regression statistics (slope, intercept, r^2) are indicated in each plot, confidence intervals are indicated in gray and all p-values ≤.05.

material, Figure S2) and EV (supplementary material, Figure S3). The width measurements (i.e., cerebral hemispheres, optic lobes, cerebellum, and inner ear regions) increase slower than EL (Table 4), reflecting the narrowing and elongation of the endocast throughout ontogeny.

The endocast of *C. brasiliensis* generally plots within the linear regressions of *S. punctatus* between the two

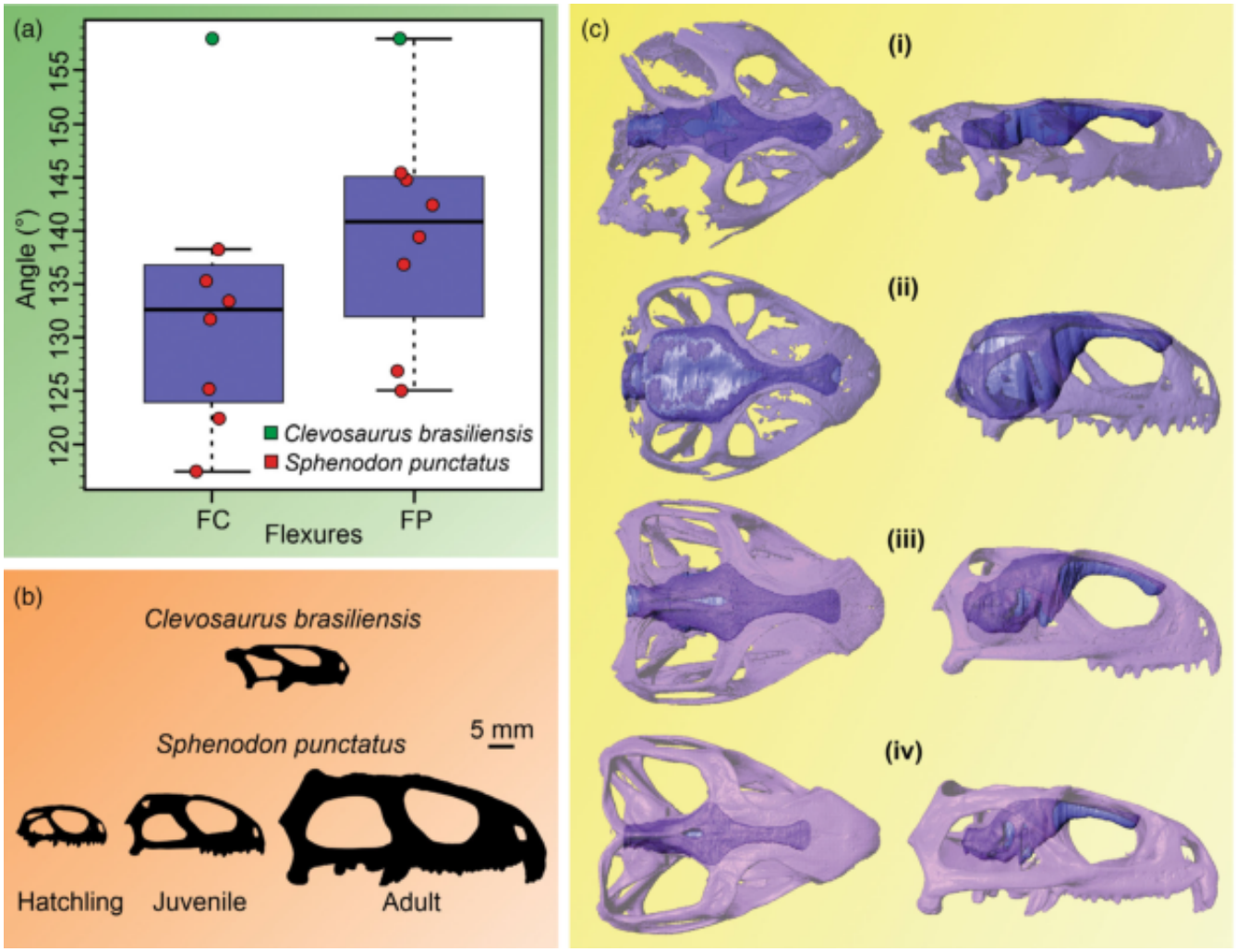

FIGURE 7 (a). Boxplot with the angle of the flexures of the endocasts of *Sphenodon punctatus* (red) and *Clevosaurus brasiliensis* (green). FC, cephalic flexure; FP, pontine flexure. (b) Outlines to scale of the lateral view of the skulls of adult *C. brasiliensis* and three *S. punctatus* in different ontogenetic stages. (c) Skull and endocast of *C. brasiliensis* (i, MCN PV 2852) and a hatchling (ii, LDUCZ x1126), a juvenile (iii, KCLZJ 001), and an adult (iv, specimen LDUCZ x036) of *S. punctatus* in dorsal (first column) and lateral (second column) views (not to scale).

hatchlings and the juvenile (closer to the former), for example, skull length versus EL, OTL, and HML (Figure 6a,c,e); endocast length versus OTL, HML, and CHW (cerebral hemispheres width) (Figure 6b,b,f); and EV versus EL, OTL, OBH (olfactory bulbs height), HML and CHW (supplementary material, Figure S3). These results show that the endocast of *C. brasiliensis* is similar, in size and inner proportions, to the expected for a juvenile of *S. punctatus* of the same size. However, most of the width measurements—brain stem anterior width, brain stem maximum width, and IEW—are proportionally smaller in the fossil specimen compared to a juvenile of *S. punctatus* (Figure 6g,h; Table 4; supplementary material, Figure S4). Regarding the width/length proportions of the endocast, *C. brasiliensis* is closer to the adults of *S. punctatus* (Table 4). Thus, the endocast of *C. brasiliensis* is short as in the juveniles of *S. punctatus* but narrow as in its adults. Additionally, the EV of *C. brasiliensis* is lower concerning skull size compared to *S. punctatus* (Table 4).

3.6 | Reptilian encephalization quotient

The body mass predictions resulted in mid-point values between 5.7 g (smaller hatchling) and 717.4 g (larger adult) for *S. punctatus* and 53.9 g for *C. brasiliensis*. The REQ values for *S. punctatus* vary from 0.666 to 1.156 (smaller to bigger specimens) with a BEC of 0.3 (REQ30%, the proportion found here), and from 1.11 to 1.926 with a BEC of 0.5 (REQ50%). The REQ30% and REQ50% of *C. brasiliensis* are 0.27 and 0.45, respectively. For complete results of body mass estimation and REQ values, see Table 5.

TABLE 5 Brain mass, body mass, and REQ of *Sphenodon punctatus* and *Clevosaurus brasiliensis*

Specimen	MBr30%	MBr50%	MBd lwr.	MBd mid.	MBd upr.	REQ30%	REQ50%
LDUCZ x1126	0.027 g	0.045 g	3.741 g	5.721 g	8.749 g	0.666	1.110
CM 30660	0.033 g	0.054 g	5.861 g	8.603 g	12.628 g	0.643	1.072
KCLZJ 001	0.156 g	0.261 g	81.204 g	93.952 g	108.702 g	0.830	1.383
SU1	0.356 g	0.593 g	390.522 g	406.863 g	423.889 g	0.842	1.404
YPM HERR 009194	0.398 g	0.663 g	410.537 g	428.276 g	446.781 g	0.915	1.526
SAMA 70524	0.405 g	0.675 g	372.312 g	387.636 g	403.591 g	0.985	1.642
LDUCZ x0036	0.667 g	1.111 g	664.491 g	717.411 g	774.546 g	1.156	1.926
MCN-PV 2852	0.037 g	0.062 g	44.090 g	53.875 g	65.831 g	0.270	0.450

Note: Both REQs were always calculated using MBd mid.
Abbreviations: MBr30%, brain mass estimated from 0.3 (30%) of endocast volume; MBr50%, brain mass estimated from 0.5 (50%) of endocast volume; MBd lwr., lower limit of body mass prediction; MBd mid., mid-point body mass prediction; MBd upr., upper limit of body mass prediction; REQ30%, Reptilian Encephalization Quotient calculated with MBr30%; REQ50%, Reptilian Encephalization Quotient calculated with MBr50%.

4 | DISCUSSION

4.1 | The brain and endocast of *S. punctatus*

The degree to which the brain occupies its cavity varies greatly among vertebrates and even among non-avian reptiles, given that it is surrounded by other structures such as meninges, cranial nerves, and blood vessels (Early et al., 2020; Hopson, 1979; Hurlburt et al., 2013; Jerison, 1973, 1977; Kim & Evans, 2014; Kotrschal et al., 1998; Northcutt, 2002). For adult crocodylians, this correspondence can be as low as 0.32 (Hurlburt et al., 2013). A comparative assessment with 15 species of squamates found a range between 0.35 (*Gekko gecko*) and 0.97 (*Callopistes maculatus*), with a mean of 0.7 (Kim & Evans, 2014). Perez-Martinez & Leal, 2021 found a sizable difference in BEC between two species of gecko (0.36 and 0.61), attributing this result to the miniaturization of the species with a higher BEC.

For *S. punctatus*, the correspondence has been reported to be low (Dendy, 1911), but to which exact degree was still untested. We corroborate that the endocast largely overestimates the brain volume in the species, founding a value on the lower end for lepidosaurs (0.3). It cannot be discarded that the brain-to-endocast relationship varies among rhynchocephalians. The BEC found for *S. punctatus* may differ for fossil species such as *C. brasiliensis*. For instance, it has been reported that miniaturized species (such as *C. brasiliensis*) can exhibit higher BEC as a possible response to the reorganization of skull bones and the need to fit more neural tissue inside small brain cavities (Ocampo et al., 2018; Perez-Martinez & Leal, 2021). Nevertheless, the value provided here is an empirical assessment of the only living species of the clade, and thus it could give closer predictions of brain size in other rhynchocephalians.

The proximity between the brain and endocast surfaces varies depending on the brain region. The dorsal surface of the hindbrain and midbrain is particularly discordant, likely due to the thicker subdural space (below the dura mater) in the dorsal region of the brain cavity (Dendy, 1911). In life, this space is filled with many connective ligaments that suspend the brain, connecting the dura and pia mater and the pineal sac between the cerebral hemispheres and the optic lobes (Dendy, 1911). The lateral "wings" of the dorsal region of the endocast that develop during ontogeny probably correspond to the thickening of the brain's cartilaginous envelopment. The existence of such structures in the endocast of *C. brasiliensis* could result from a similar phenomenon, so these "wings" are likely also not brain structures in the species.

Nevertheless, the endocast reflects the brain's general shape and some length measurements in *S. punctatus*. The olfactory tract, the cerebral hemispheres' dorsal surface, and the pituitary's ventral limit seem to be closer to the brain than the optic lobes and cerebellum region. A closer correspondence of the forebrain in comparison to other brain subdivisions is also seen in crocodylians (Dumont et al., 2020; Watanabe et al., 2019). Squamates also exhibit the general pattern of the olfactory bulbs, olfactory tract, and cerebral hemispheres (plus the medulla oblongata) being the most discernible brain regions from the endocasts, with the cerebellum region being the least discernible (Allemand et al., 2023). Reports on a wide range of vertebrates show a considerable variation in the spatial relationship of the brain and brain cavity between neuroanatomical regions (Allemand et al., 2023; Challands et al., 2020; Clement et al., 2021;

Dumont et al., 2020; Early et al., 2020; Evers et al., 2019; Jirák & Janáček, 2017; Watanabe et al., 2019). Using the total volume as the only metric for brain-to-endocast comparisons ignores this variation and can disregard the informative potential of endocasts. Although the endocast of *S. punctatus* fails to represent the volume and some features of the brain, it recovers some aspects of its morphology. Thus, we suggest that endocasts are viable tools to study neuroanatomy in fossil rhynchocephalians as long as their limitations are considered and acknowledged.

4.2 | The endocast of *C. brasiliensis*

The endocast of *C. brasiliensis* shares similar length dimensions and some anatomical features (i.e., less constricted olfactory tract and inner ear region) with juveniles of *S. punctatus*. *Clevosaurus brasiliensis* is smaller than almost all rhynchocephalians (Arantes et al., 2009; Bonaparte & Sues, 2006; Hsiou et al., 2015), with its size being comparable to that of a young juvenile of *S. punctatus*. Thus, the similarities between the fossil species and juvenile tuatara can be at least partially explained by allometry. However, details differ: the relatively narrow width of the endocast of *C. brasiliensis* and the diamond shape of its forebrain + midbrain in dorsal view are absent from hatchling tuatara and only seen in adult tuatara. Given that the endocast of *S. punctatus* was shown to particularly overestimate the width of the brain (rather than length) and that the lateral expansions responsible for the diamond shape are not directly related to the brain, the similarities shared between *C. brasiliensis* and adult tuatara may also not be a reflection of actual brain similarities. Finally, characteristics such as the very low dorsoventral angulation and the comparatively lower EV relative to skull size are unique to *C. brasiliensis* and set it apart from the living species.

Clevosaurids are considerably diverse in species and, to an extent, in cranial anatomy, including the relative size of their basicranium (Chambi-Trowell et al., 2019), which possibly affects endocast shape. Also, as stated above, miniaturization (as appears to occur in *C. brasiliensis*) can result in a reconfiguration of the skull bones, brain shape, and relative brain size (Perez-Martinez & Leal, 2021; Striedter, 2005). It is possible that investigating other *Clevosaurus* species may reveal a neuroanatomical diversity in the clade. Moreover, Clevosauridae is a relatively well nested clade with many apomorphies (DeMar Jr et al., 2022; Simões et al., 2020, 2022). Thus, despite the endocast of *C. brasiliensis* being the oldest for a rhynchocephalian (and lepidosaur) to date, its anatomy should not be regarded as the plesiomorphic condition for Rhynchocephalia.

4.3 | Brain size, encephalization, and implications

The REQ of *C. brasiliensis* (i.e., 0.27) is considerably lower than adult *S. punctatus* (i.e., 0.842–1.156), with the former bordering the lower end and the latter falling within the range of non-avian reptiles (Hurlburt et al., 2013). The ontogenetic REQ increase in *S. punctatus* shows the opposite tendency of other non-avian reptiles (Hurlburt et al., 2013). However, encephalization can be underestimated if brain mass is being so. Given that BEC can decrease drastically throughout ontogeny in other non-avian reptiles (Hurlburt et al., 2013; Jirák & Janáček, 2017; Watanabe et al., 2019), this likely occurs in *S. punctatus* as well. Therefore, we believe the brain mass values for immature specimens found here are likely underestimations, thus creating artificially lower REQ values.

The REQ50% (being that 0.5 is the approximate BEC of intermediate-sized alligators; Hurlburt et al., 2013) is slightly higher in KCLZJ 001 (i.e., 1.383), the medium-sized juvenile in our sample, than the REQ30% of adult specimens (i.e., 0.842–1.156). As for the hatchlings, if a BEC of 0.97 (the value found for younger *A. mississippiensis*; Watanabe et al., 2019) is used, the REQ of the smaller specimen (LDUCZ x1126) would go up to 2.154. Therefore, it is plausible that the REQ also decreases throughout *S. punctatus* ontogeny, but this assumption can only be supported if the brain masses of younger specimens are obtained (through direct weighting or investigation of their brain-to-endocast ratio). This would likely allow a more accurate analysis of the REQ of *S. punctatus* in different stages of life and non-adult fossil specimens.

Criticism of encephalization quotients and alternative measures of brain size and efficiency have been raised (Butler & Hodos, 1996; Font et al., 2019; Herculano-Houzel et al., 2014; Smaers & Soligo, 2013; Striedter, 2005; van Schaik et al., 2021). Still, several studies show that brain size (total or partial) can be correlated to the evolution of sensory systems, behavioral plasticity, and social complexity (Jerison, 1973, 1977; Northcutt, 2002; Striedter, 2005). The brain is a very metabolically costly organ, so it is likely that the increase in its size and complexity may be related to its function (Heldstab et al., 2022; Northcutt, 2002, 2013). The tuatara does exhibit complex social behaviors, fast visual discrimination, and learning capabilities (Font et al., 2019; Gillingham et al., 1995; Northcutt, 2013; Northcutt & Heath, 1973). Although a tendency to increase in encephalization is seen in other clades (Balanoff et al., 2013; Dumont et al., 2020; Lautenschlager et al., 2018), inferences regarding encephalization evolutionary trends in Rhynchocephalia

require analysis of further fossil species. Additionally, it is important to reiterate that the brain volume of *C. brasiliensis* (as in other fossil species) is an estimation, and factors such as the lack of bony surroundings and clear osteological landmarks for some regions, as well as the possibility of a different BEC than *S. punctatus*, could affect REQ calculations.

4.4 | Ontogenetic variation, allometric relationships, and heterochrony

Although the ontogeny of *S. punctatus* is somewhat known (Dendy, 1899; Howes & Swinnerton, 1901; Jones, 2008; Jones et al., 2011; Rieppel, 1992; Robinson, 1976), the development of its brain cavity is poorly studied (but see Dendy, 1911 for brief discussions for the early life stages of the species). Throughout development, the volume of the endocast of *S. punctatus* increases linearly with skull size, but its shape varies considerably: it becomes narrower, longer, and less dorsoventrally curved. The elongation of the hindbrain and olfactory tract reflects the elongation of the preorbital region and decrease of relative orbit size (Howes & Swinnerton, 1901; Rieppel, 1992), patterns that are widespread among vertebrates (Dumont et al., 2020; Hu et al., 2021; Jirák & Janáček, 2017; Lautenschlager & Hübner, 2013; Macrini et al., 2007; Watanabe et al., 2019).

The flexure of the endocast decreases with ontogeny in *S. punctatus*, while in adult *C. brasiliensis*, it is strikingly low and outside the range of the living species (Figure 7). An ontogenetic reduction in brain angulation is seen in many other taxa, mostly non-avian reptiles (Dumont et al., 2020; Hu et al., 2021; Jirák & Janáček, 2017; Lautenschlager et al., 2018; Lautenschlager & Hübner, 2013). This pattern also reflects changes in skull shape, such as the flattening of the skull roof, the elongation of the preorbital region, and the decrease in relative orbit size (Figure 7) (Fabbri et al., 2017; Lautenschlager & Hübner, 2013). Straighter and more tubular brains are generally considered a plesiomorphic condition within clades and have been associated with less complex and/or specialized brains (Jerison, 1973). In turtles and crocodylians, some fossil species present a more linear brain cavity than their living relatives (Dumont et al., 2020; Lautenschlager et al., 2018). These observations hint that *C. brasiliensis* may show a plesiomorphic condition relative to *S. punctatus*. However, this pattern is not universal; for instance, within phytosaurs, some of the most nested species show the lowest angulation (Lautenschlager & Butler, 2016). Ultimately, further endocasts of early lepidosaurs and lepidosauromorphs are required to understand these evolutionary trends better.

Many ontogenetic changes that the skull of *S. punctatus* undergoes throughout ontogeny echo what occurs during rhynchocephalian evolution (Jones, 2008). For instance, during *S. punctatus* ontogeny, the postorbital area of the skull expands relative to the orbital and preorbital regions (Howes & Swinnerton, 1901; Jones, 2008; Rieppel, 1992). Comparatively, the postorbital area is shorter in non-eusphenodontians (i.e., *Diphydontosaurus avonis*, *Gephyrosaurus bridensis*, and *Planocephalosaurus robinsonae*) (Evans, 1980; Fraser, 1988; Whiteside, 1986; Wu, 2003) and longer in more derived lineages such as clevosaurs, eilenodontines, and sphenodontines (Apesteguía & Novas, 2003; Arantes et al., 2009; Bonaparte & Sues, 2006; Fraser, 1988; Fraser & Benton, 1989; Meloro & Jones, 2012; Sues et al., 1994). The skull roof is flat in early hatchlings of tuatara, forming a tall parietal crest during development (Dendy, 1899; Rieppel, 1992). Similarly, the skull roof is broad and flat in many early divergent rhynchocephalians such as *G. bridensis*, *P. robinsonae*, *Polysphenodon mulleri*, and *D. avonis* (Carroll, 1985; Evans, 1980; Fraser, 1982; Whiteside, 1986), narrower but still flat in clevosaurs (e.g., Bonaparte & Sues, 2006; Fraser, 1988), and organized in a parietal crest in more derived terrestrial species such as *Zapatodon ejidoensis*, *Kallimodon pulchellus*, *Sapheosaurus thiollierei*, *Priosphenodon avelasi*, and *S. punctatus* (Apesteguía & Novas, 2003; Jones, 2008).

These patterns may indicate that the cranial morphology of *S. punctatus* is peramorphic in relation to many fossil rhynchocephalians since it develops "beyond" what occurs in them (McNamara, 2012). The high longevity and late sexual maturity of *S. punctatus* are characteristics typically associated with hypermorphosis (a type of peramorphosis where the growth period of a species is extended concerning ancestral lineages). Given that heterochrony usually leads to change in the allometric relationships of organisms (McNamara, 2012), the similarities between the endocast of *C. brasiliensis* and juveniles of *S. punctatus* could be a combination of allometric and heterochronic factors. Nevertheless, it is important to reiterate that *C. brasiliensis* is a very small rhynchocephalian with particularly juvenile-like cranial characteristics (in the context of *S. punctatus*) that affect endocast shape (e.g., extremely short snout and very large orbits), which could be emphasizing a possible peramorphic endocast anatomy in *S. punctatus*.

5 | CONCLUSION

This work presents the first description of the endocast of a fossil rhynchocephalian to date and the first comparative examination of endocast anatomy in the clade. In summary, we observed that: (a) the endocast of *S. punctatus*

does not reflect the volume and detailed morphology of the brain, but it recovers its general form and length; (b) the REQ of *S. punctatus* is slightly on the lower end for non-avian reptiles, and the REQ of *C. brasiliensis* is considerably lower; (c) the endocast of *S. punctatus* changes throughout ontogeny in a way that reflects the skull shape and with patterns similar to those of other non-avian reptiles (i.e., elongation, narrowing, and linearization); and (d) the endocast of *C. brasiliensis* has similarities in size and shape with *S. punctatus*, especially young juveniles, but it also presents unique features such as a more linear and less dorsoventrally flexed organization and lower relative volume. We also present an empirical BEC value for the tuatara, assisting brain size estimations in fossil rhynchocephalians. Our results suggest that allometric and possibly heterochronic phenomena play a role in the morphological diversity of the rhynchocephalian brain cavity. By providing the oldest endocast of a lepidosaur to date and adding information regarding the anatomy and ontogeny of the brain cavity of the only living rhynchocephalian, this study expands the anatomical knowledge of the clade and contributes to future investigations of its neuroanatomical patterns.

AUTHOR CONTRIBUTIONS

Lívia Roese-Miron: Investigation; writing – original draft; methodology; visualization; writing – review and editing; formal analysis; funding acquisition; conceptualization. **Marc Emyr Huw Jones:** Conceptualization; writing – review and editing; supervision; resources; funding acquisition; methodology. **José Darival Ferreira:** Writing – review and editing; visualization. **Annie Schmaltz Hsiou:** Conceptualization; funding acquisition; supervision; resources.

ACKNOWLEDGMENTS

The authors thank Mark Hutchinson, Paul Scofield, Anton Maksimenko, Jacques Gauthier, Jay Richard Black, Joey Gerlach, Jessie Maisano, John Hutchinson, Matthew Colbert, Richard Ketcham, Sophie Regnault, Sue Taft, Susan Evans, Tim Rowe, and Zerina Johansen for help accessing and/or scanning the specimens of *S. punctatus*, and Ana Maria Ribeiro for help accessing the specimen of *C. brasiliensis*. The authors would also like to thank DigiMorph (digimorph.org), from which two *S. punctatus* specimens were accessed, Allison Cree for sharing a body mass dataset for *S. punctatus*, Natalie Cooper for providing the R script to calculate body mass estimates, and the Australian Synchrotron for funding. Finally, the authors thank the reviewers Gabriela Sobral and an anonymous reviewer for their valuable contributions to this article.

CONFLICT OF INTEREST

The authors declare no conflicts of interest.

DATA AVAILABILITY STATEMENT

The 3D surface models of the brain, brain cavity, endosseous labyrinth, and initial trunks of the cranial nerves generated by this study are available in the online repository MorphoMuseuM (morphomuseum.co) (doi: 10.18563/journal.m3.185), as well as 3D PDF files in the Supplementary Material. The R code and additional data necessary to replicate the analyses are also available in the Supplementary Material.

ORCID

Lívia Roese-Miron https://orcid.org/0000-0002-2722-4528
Marc Emyr Huw Jones https://orcid.org/0000-0002-0146-9623
José Darival Ferreira https://orcid.org/0000-0002-2779-6120
Annie Schmaltz Hsiou https://orcid.org/0000-0003-2392-6191

REFERENCES

Abbie, A. A. (1934). The morphology of the fore-brain arteries, with especial reference to the evolution of the basal ganglia. *Journal of Anatomy*, *68*(4), 433.

Abdala, F., & Giannini, N. P. (2000). Gomphodont cynodonts of the Chañares formation: The analysis of an ontogenetic sequence. *Journal of Vertebrate Paleontology*, *20*(3), 501–506.

Allemand, R. (2017). *Etude microtomographique de l'endocrâne de reptiles marins (Plesiosauria et Mosasauroidea) du Turonien (Crétacé supérieur) du Maroc: Implications paléobiologiques et comportementales* (Doctoral Thesis). Muséum National d'Histoire Naturelle, Paris, France.

Allemand, R., Abdul-Sater, J., Macrì, S., Di-Poï, N., Daghfous, G., & Silcox, M. T. (2023). Endocast, brain, and bones: Correspondences and spatial relationships in squamates. *The Anatomical Record*, 1–23.

Allemand, R., Boistel, R., Daghfous, G., Blanchet, Z., Cornette, R., Bardet, N., Vincent, P., & Houssaye, A. (2017). Comparative morphology of snake (Squamata) endocasts: Evidence of phylogenetic and ecological signals. *Journal of Anatomy*, *231*(6), 849–868.

Anantharaman, S., Demar, D. G., Jr., Sivakumar, R., Dassarma, D. C., Wilson Mantilla, G. P., & Wilson Mantilla, J. A. (2022). First rhynchocephalian (Reptilia, Lepidosauria) from the Cretaceous–Paleogene of India. *Journal of Vertebrate Paleontology*, *42*(1), e2118059.

Andreis, R. R., Cazzulo-Klepzig, M., Guerra-Sommer, M., & Zimermann, L. (1980). Considerações sobre um afloramento fossilífero do Grupo Itararé: Fazenda Goulart, Francisquinho, município de São Jerônimo, RS. *Boletim IG*, *11*, 85–97.

Apesteguía, S., & Carballido, J. L. (2014). A new eilenodontine (Lepidosauria, Sphenodontidae) from the Lower Cretaceous of

central Patagonia. *Journal of Vertebrate Paleontology*, *34*, 303–317.

Apesteguía, S., Garberoglio, F. F., & Gómez, R. O. (2021). Earliest tuatara relative (Lepidosauria: Sphenodontinae) from southern continents. *Ameghiniana*, *58*(5), 416–441.

Apesteguía, S., Gómez, R. O., & Rougier, G. W. (2012). A basal sphenodontian (Lepidosauria) from the Jurassic of Patagonia: New insights on the phylogeny and biogeography of Gondwanan rhynchocephalians. *Zoological Journal of the Linnean Society*, *166*, 342–360.

Apesteguía, S., Gómez, R. O., & Rougier, G. W. (2014). The youngest South American rhynchocephalian, a survivor of the KPg extinction. *Proceedings of the Royal Society B*, *281*, 1–6.

Apesteguía, S., & Jones, M. E. H. (2012). A Late Cretaceous tuatara (Lepidosauria: Sphenodontinae) from South America. *Cretaceous Research*, *34*, 154–160.

Apesteguía, S., & Novas, F. E. (2003). Large Cretaceous sphenodontian from Patagonia provides insight into lepidosaur evolution in Gondwana. *Nature*, *425*, 609–612.

Arantes, B., Soares, M., & Schultz, C. (2009). *Clevosaurus brasiliensis* (Lepidosauria, Sphenodontia) do Triássico Superior do Rio Grande do Sul: anatomia pós-craniana e relações filogenéticas. *Revista Brasileira de Paleontologia*, *12*, 43–54.

Balanoff, A. M., & Bever, G. S. (2017). The role of endocasts in the study of brain evolution. In J. H. Kaas (Ed.), *Evolution of nervous systems* (2nd ed., pp. 223–241). Academic Press.

Balanoff, A. M., Bever, G. S., Colbert, M. W., Clarke, J. A., Field, D. J., Gignac, P. M., Ksepka, D. T., Ridgely, R. C., Smith, N. A., Torres, C. R., Walsh, S., & Witmer, L. M. (2016). Best practices for digitally constructing endocranial casts: Examples from birds and their dinosaurian relatives. *Journal of Anatomy*, *229*, 173–190.

Balanoff, A. M., Bever, G. S., Rowe, T. B., & Norell, M. A. (2013). Evolutionary origins of the avian brain. *Nature*, *501*(7465), 93–96.

Bever, G. S., Bell, C. J., & Maisano, J. A. (2005). The ossified braincase and cephalic osteoderms of Shinisaurus crocodilurus (Squamata, Shinisauridae). *Palaeontologia Electronica*, *8*(1), 1–36.

Bisconti, M., Damarco, P., Tartarelli, G., Pavia, M., & Carnevale, G. (2021). A natural endocast of an early Miocene odontocete and its implications in cetacean brain evolution. *The Journal of Comparative Neurology*, *529*(6), 1198–1227.

Bonaparte, J. F., Ferigolo, J., & Ribeiro, A. M. (1999). A new early Late Triassic Saurischian dinosaur from Rio Grande do Sul state, Brazil. *National Science Museum Monographs*, *15*, 89–109.

Bonaparte, J. F., Schultz, C. L., Soares, M. B., & Martinelli, A. G. (2010). La fauna local de Faxinal do Soturno, Triásico Tardío de Rio Grande do Sul. *Revista Brasileira de Paleontologia*, *13*(3), 233–246.

Bonaparte, J. F., & Sues, H. D. (2006). A new species of *Clevosaurus* (Lepidosauria: Rhynchocephalia) from the Upper Triassic of Rio Grande Do Sul, Brazil. *Palaeontology*, *49*, 917–923.

Burbrink, F. T., Grazziotin, F. G., Pyron, R. A., Cundall, D., Donnellan, S., Irish, F., Keogh, J. S., Kraus, F., Murphy, R. W., Noonan, B., Raxworthy, S. R., Lemmon, A. R., Lemmon, E. M., & Zaher, H. (2020). Interrogating genomic-scale data for Squamata (lizards, snakes, and Amphisbaenians) shows no support for key traditional morphological relationships. *Systematic Biology*, *69*(3), 502–520.

Butler, A., & Hodos, W. (1996). *Comparative vertebrate neuroanatomy: Evolution and adaptation* (2nd ed.). John Wiley and Sons.

Camp, C. L. (1942). *California mosasaurs*. University of California Press.

Carril, J., Tambussi, C. P., Degrange, F. J., Benitez Saldivar, M. J., & Picasso, M. B. J. (2016). Comparative brain morphology of Neotropical parrots (Aves, Psittaciformes) inferred from virtual 3D endocasts. *Journal of Anatomy*, *229*(2), 239–251.

Carroll, R. L. (1985). A pleurosaur from the Lower Jurassic and the taxonomic position of the Sphenodontia. *Palaeontographica Abteilung A*, *189*, 1–28.

Castanet, J., Newman, D. G., & Girons, H. S. (1988). Skeletochronological data on the growth, age, and population structure of the tuatara, *Sphenodon punctatus*, on Stephens and Lady Alice Islands, New Zealand. *Herpetologica*, *44*(1), 25–37.

Challands, T. J., Pardo, J. D., & Clement, A. M. (2020). Mandibular musculature constrains brain-endocast disparity between sarcopterygians. *Royal Society Open Science*, *7*(9), 200933.

Chambi-Trowell, S. A., Martinelli, A. G., Whiteside, D. I., Vivar, P. R. R. D., Soares, M. B., Schultz, C. L., Gill, P. G., Benton, M. J., & Rayfield, E. J. (2021). The diversity of Triassic South American sphenodontians: A new basal form, clevosaurs, and a revision of rhynchocephalian phylogeny. *Journal of Systematic Palaeontology*, *19*, 1–34.

Chambi-Trowell, S. A., Whiteside, D. I., & Benton, M. J. (2019). Diversity in rhynchocephalian *Clevosaurus* skulls based on CT reconstruction of two Late Triassic species from Great Britain. *Acta Palaeontologica Polonica*, *64*(1), 41–64.

Christensen, K. (1927). The morphology of the brain of *Sphenodon*. *University of Iowa Museum of Natural History*, *12*, 1–29.

Christiansen, P., & Fariña, R. A. (2004). Mass prediction in theropod dinosaurs. *Historical Biology*, *16*, 85–92.

Clement, A. M., Mensforth, C. L., Challands, T. J., Collin, S. P., & Long, J. A. (2021). Brain reconstruction across the fish-tetrapod transition: Insights from modern amphibians. *Frontiers in Ecology and Evolution*, *9*, 160.

Cooper, N., & Purvis, A. (2009). What factors shape rates of phenotypic evolution? A comparative study of cranial morphology of four mammalian clades. *Journal of Evolutionary Biology*, *22*(5), 1024–1035.

Corfield, J. R., Wild, J. M., Parsons, S., & Kubke, M. F. (2012). Morphometric analysis of telencephalic structure in a variety of neognath and paleognath bird species reveals regional differences associated with specific behavioral traits. *Brain, Behavior and Evolution*, *80*(3), 181–195.

Cree, A. (2014). Reproductive anatomy and cycles of tuatara (*Sphenodon punctatus*), an intriguing non-squamate lepidosaur. In J. L. Rheubert, D. S. Siegel, & S. E. Trauth (Eds.), *Reproductive biology and phylogeny of lizards and tuatara* (pp. 620–646). CRC Press.

Cree, A., Cockrem, J. F., & Guillette, L. J. (1992). Reproductive cycles of male and female tuatara (*Sphenodon punctatus*) on Stephens Island, New Zealand. *Journal of Zoology*, *226*, 199–211.

Cree, A., Guillette, L. J., Brown, M. A., Chambers, G. K., Cockrem, J. F., & Newton, J. D. (1991). Slow estradiol-induced

Vitellogenesis in the tuatara, *Sphenodon punctatus*. *Physiological Zoology*, *64*(5), 1234–1251.

Cuthbertson, R. S., Maddin, H. C., Holmes, R. B., & Anderson, J. S. (2015). The braincase and endosseous labyrinth of *Plioplatecarpus peckensis* (Mosasauridae, Plioplatecarpinae), with functional implications for locomotor behavior. *The Anatomical Record*, *298*, 1597–1611.

DeMar, D. G., Jr., Jones, M. E., & Carrano, M. T. (2022). A nearly complete skeleton of a new eusphenodontian from the Upper Jurassic Morrison Formation, Wyoming, USA, provides insight into the evolution and diversity of Rhynchocephalia (Reptilia: Lepidosauria). *Journal of Systematic Palaeontology*, *20*(1), 2093139.

Dempster, W. T. (1935). The brain case and endocranial cast of *Eryops megacephalus*. *The Journal of Comparative Neurology*, *62*(1), 171–196.

Dendy, A. (1899). Outlines of the development of the tuatara, *Sphenodon* (*Hatteria*) *punctatus*. *The Quarterly Journal of Microscopical Science*, *42*, 1–72.

Dendy, A. (1909). X. The intracranial vascular system of *Sphenodon*. *Philosophical Transactions of the Royal Society of London. Series B, Biological Sciences*, *200*(262–273), 403–426.

Dendy, A. (1911). On the structure, development and morphological interpretation of the pineal organs and adjacent parts of the brain in the tuatara (*Sphenodon punctatus*). *Philosophical Transactions of the Royal Society of London B. Series B, Biological Sciences*, *201*, 226–331.

Dozo, M. T., Paulina-Carabajal, A., Macrini, T. E., & Walsh, S. (Eds.). (2022). *Paleoneurology of amniotes: New directions in the study of fossil endocasts*. Springer Nature.

Dufeau, D. L., & Witmer, L. M. (2015). Ontogeny of the middle-ear air-sinus system in *Alligator mississippiensis* (Archosauria: Crocodylia). *PLoS One*, *10*(9), e0137060.

Dumont, M. V., Jr., Santucci, R. M., de Andrade, M. B., & de Oliveira, C. E. M. (2020). Paleoneurology of *Baurusuchus* (Crocodyliformes: Baurusuchidae), ontogenetic variation, brain size, and sensorial implications. *The Anatomical Record*, *305*(10), 1–25.

Durward, A. (1930). The cell masses in the forebrain of *Sphenodon punctatum*. *Journal of Anatomy*, *65*(1), 8–44.

Early, C. M., Iwaniuk, A. N., Ridgely, R. C., & Witmer, L. M. (2020). Endocast structures are reliable proxies for the sizes of corresponding regions of the brain in extant birds. *Journal of Anatomy*, *237*(6), 1162–1176.

Edinger, T. (1951). The brains of the Odontognathae. *Evolution*, *5*(1), 6–24.

Evans, S. E. (1980). The skull of a new eosuchian reptile from the lower Jurassic of South Wales. *Zoological Journal of the Linnean Society*, *70*(3), 203–264.

Evans, S. E. (2003). At the feet of the dinosaurs: The early history and radiation of lizards. *Biological Reviews*, *78*(4), 513–551.

Evans, S. E. (2016). The lepidosaurian ear: Variations on a theme. In J. A. Clack, R. R. Fay, & A. N. Popper (Eds.), *Evolution of the vertebrate ear* (pp. 245–284). Springer International Publishing.

Evans, S. E., & Jones, M. E. H. (2010). The origin, early history and diversification of lepidosauromorph reptiles. In *New aspects of Mesozoic biodiversity* (pp. 27–44). Springer Berlin.

Evers, S. W., Neenan, J. M., Ferreira, G. S., Werneburg, I., Barrett, P. M., & Benson, R. B. (2019). Neurovascular anatomy of the protostegid turtle *Rhinochelys pulchriceps* and comparisons of membranous and endosseous labyrinth shape in an extant turtle. *Zoological Journal of the Linnean Society*, *187*(3), 800–828.

Fabbri, M., Koch, N. M., Pritchard, A. C., Hanson, M., Hoffman, E., Bever, G. S., Balanoff, A. M., Morris, Z. S., Field, D. J., Camacho, J., Rowe, T. B., Norell, M. A., Smith, R. M., Abzhanov, A., & Bhullar, B-A. S. (2017). The skull roof tracks the brain during the evolution and development of reptiles including birds. *Nature Ecology and Evolution*, *1*(10), 1543–1550.

Farlow, J. O., Hurlburt, G. R., Elsey, R. M., Britton, A. R., & Langston, W., Jr. (2005). Femoral dimensions and body size of *Alligator mississippiensis*: Estimating the size of extinct mesoeucrocodylians. *Journal of Vertebrate Paleontology*, *25*(2), 354–369.

Ferreira, J. D., Dozo, M. T., Bubadué, J. M., & Kerber, L. (2022). Morphology and postnatal ontogeny of the cranial endocast and paranasal sinuses of capybara (*Hydrochoerus hydrochaeris*), the largest living rodent. *Journal of Morphology*, *283*(1), 66–90.

Font, E., García-Roa, R., Pincheira-Donoso, D., & Carazo, P. (2019). Rethinking the effects of body size on the study of brain size evolution. *Brain, Behavior and Evolution*, *93*(4), 182–195.

Franco, A. S., Müller, R. T., Martinelli, A. G., Hoffmann, C. A., & Kerber, L. (2021). The nasal cavity of two traversodontid cynodonts (Eucynodontia, Gomphodontia) from the Upper Triassic of Brazil. *Journal of Paleontology*, *95*(4), 845–860.

Fraser, N. C. (1982). A new rhynchocephalian from the British Upper Trias. *Palaeontology*, *25*, 709–725.

Fraser, N. C. (1988). The osteology and relationships of *Clevosaurus* (Reptilia: Sphenodontida). *Philosophical Transactions of the Royal Society of London. Series B, Biological Sciences*, *321*, 125–178.

Fraser, N. C., & Benton, M. J. (1989). The Triassic reptiles *Brachyrhinodon* and *Polysphenodon* and the relationships of the sphenodontids. *Zoological Journal of the Linnean Society*, *96*(4), 413–445.

Gans, C., & Wever, E. G. (1976). Ear and hearing in *Sphenodon punctatus*. *PNAS*, *73*(11), 4244–4246.

Gemmell, N. J., Rutherford, K., Prost, S., Tollis, M., Winter, D., Macey, J. R., Adelson, D. L., Suh, A., Bertozzi, T., Grau, J. H., Organ, C., Gardner, P. P., Muffato, M., Patricio, M., Billis, K., Martin, F., J., Flicek, P., Petersen, B., Kang, L., ... Board, N. T. (2020). The tuatara genome reveals ancient features of amniote evolution. *Nature*, *584*(7821), 403–409.

Gignac, P. M., & Kley, N. J. (2018). The utility of diceCT imaging for high-throughput comparative neuroanatomical studies. *Brain, Behavior and Evolution*, *91*, 180–190.

Gignac, P. M., Kley, N. J., Clarke, J. A., Colbert, M. W., Morhardt, A. C., Cerio, D., Cost, I. N., Cox, P. G., Daza, J. D., Early, C. M., Echols, M. S., Henkelman, R. M., Herdina, A. N., Holliday, C. M., Li, Z., Mahlow, K., Merchant, S., Müller, J., Orsbon, C. P., ... Witmer, L. M. (2016). Diffusible iodine-based contrast- enhanced computed tomography (diceCT): An emerging tool for rapid, high-resolution, 3-D imaging of metazoan soft tissues. *Journal of Anatomy*, *228*(6), 889–909.

Gillingham, J. C., Carmichael, C., & Miller, T. (1995). Social behavior of the tuatara, *Sphenodon punctatus*. *Herpetological Monographs*, *9*, 5–16.

Gingerich, P. D. (1990). Prediction of body mass in mammalian species from long bone lengths and diameters. *Contributions from the Museum of Paleontology*, *28*(4), 79–92.

Hammer, Ø., Harper, D. A. T., & Ryan, P. D. (2001). PAST: Paleontological statistics software package for education and data analysis. *Palaeontologia Electronica*, *4*(1), 1–9.

Harrison, H. S. (1901). *Hatteria punctatae* its dentitions and its incubation period. *Anatomischer Anzeiger*, *20*, 145–158.

Heldstab, S. A., Isler, K., Graber, S. M., Schuppli, C., & van Schaik, C. P. (2022). The economics of brain size evolution in vertebrates. *Current Biology*, *32*, R697–R708.

Herculano-Houzel, S., Manger, P. R., & Kaas, J. H. (2014). Brain scaling in mammalian evolution as a consequence of concerted and mosaic changes in numbers of neurons and average neuronal cell size. *Frontiers in Neuroanatomy*, *8*, 77.

Herrera-Flores, J. A., Elsler, A., Stubbs, T. L., & Benton, M. J. (2022). Slow and fast evolutionary rates in the history of lepidosaurs. *Palaeontology*, *65*(1), e12579.

Herrera-Flores, J. A., Stubbs, T. L., & Benton, M. J. (2017). Macroevolutionary patterns in Rhynchocephalia: Is the tuatara (*Sphenodon punctatus*) a living fossil? *Palaeontology*, *60*(3), 319–328.

Herrera-Flores, J. A., Stubbs, T. L., Elsler, A., & Benton, M. J. (2018). Taxonomic reassessment of *Clevosaurus latidens* Fraser, 1993 (Lepidosauria, Rhynchocephalia) and rhynchocephalian phylogeny based on parsimony and Bayesian inference. *Journal of Paleontology*, *92*, 734–742.

Hindenach, J. C. R. (1931). The cerebellum of *Sphenodon punctatum*. *Journal of Anatomy*, *65*(3), 283–318.

Holloway, R. L. (2018). On the making of endocasts: The new and the old in paleoneurology. In E. Bruner, N. Ogihara, H. C. Tanabe (Eds.), *Digital endocasts: From skulls to brains* (pp. 1–8). Springer Tokyo.

Hoops, D., Vidal-García, M., Ullmann, J. F., Janke, A. L., Stait-Gardner, T., Duchêne, D. A., Price, W. S., Whiting, M. J., & Keogh, J. S. (2017). Evidence for concerted and mosaic brain evolution in dragon lizards. *Brain, Behavior and Evolution*, *90*(3), 211–223.

Hopson, J. A. (1977). Relative brain size and behavior in archosaurian reptiles. *Annual Review of Ecology, Evolution, and Systematics*, *8*(1), 429–448.

Hopson, J. A. (1979). Paleoneurology. In C. Gans, R. G. Northcutt, & P. S. Ulinski (Eds.), *Biology of the Reptilia* (Vol. 9, pp. 39–146). Academic Press.

Horn, B. L. D., Melo, T. M., Schultz, C. L., Philipp, R. P., Kloss, H. P., & Goldberg, K. (2014). A new third-order sequence stratigraphic framework applied to the Triassic of the Paraná Basin, Rio Grande do Sul, Brazil, based on structural, stratigraphic and paleontological data. *Journal of South American Earth Sciences*, *55*, 123–132.

Howes, G. B., & Swinnerton, H. H. (1901). On the development of the skeleton of the tuatara, *Sphenodon punctatus*; with remarks on the egg, hatching, and on the hatched young. *Transactions of the Zoological Society of London*, *16*(1), 1–74.

Hsiou, A. S., França, M. A. G., & Ferigolo, J. (2015). New data on the Clevosaurus (Sphenodontia: Clevosauridae) from the Upper Triassic of Southern Brazil. *PLoS One*, *10*(9), e0137523.

Hsiou, A. S., Nydam, R. L., Simões, T. R., Pretto, F. A., Onary, S., Martinelli, A. G., Liparini, A., Romo-de-Vivar-Martínez, P. R., Soares, M. B., Schultz, C. L., & Caldwell, M. W. (2019). A new clevosaurid from the Triassic (Carnian) of Brazil and the rise of sphenodontians in Gondwana. *Scientific Reports*, *9*, 1–12.

Hu, K., King, J. L., Romick, C. A., Dufeau, D. L., Witmer, L. M., Stubbs, T. L., Rayfield, E. J., & Benton, M. J. (2021). Ontogenetic endocranial shape change in alligators and ostriches and implications for the development of the non-avian dinosaur endocranium. *The Anatomical Record*, *304*(8), 1759–1775.

Hurlburt, G. R. (1996). *Relative brain size in recent and fossil amniotes*: *Determination and interpretation* (Doctoral Thesis). University of Toronto, Toronto, Canada.

Hurlburt, G. R. (1999). Comparison of body mass estimation techniques, using recent reptiles and the pelycosaur *Edaphosaurus boanerges*. *Journal of Vertebrate Paleontology*, *19*(2), 338–350.

Hurlburt, G. R., Ridgely, R. C., & Witmer, L. M. (2013). Relative size of brain and cerebrum in tyrannosaurid dinosaurs: An analysis using brain-endocast quantitative relationships in extant alligators. In J. M. Parrish, R. E. Molnar, P. J. Currie, & E. B. Koppelhus (Eds.), *Tyrannosaurid paleobiology* (pp. 135–154). Indiana University Press.

Jerison, H. J. (1973). *Evolution of the brain and intelligence*. Academic Press.

Jerison, H. J. (1977). The theory of encephalization. *Annals of the New York Academy of Sciences*, *299*, 146–160.

Jirák, D., & Janáček, J. (2017). Volume of the crocodilian brain and endocast during ontogeny. *PLoS One*, *12*(6), e0178491.

Jones, M. E., Curtis, N., Fagan, M. J., O'Higgins, P., & Evans, S. E. (2011). Hard tissue anatomy of the cranial joints in *Sphenodon* (Rhynchocephalia): Sutures, kinesis, and skull mechanics. *Palaeontologia Electronica*, *14*(2), 17A.

Jones, M. E. H. (2006). The Early Jurassic Clevosaurs from China (Diapsida: Lepidosauria). In J. D. Harris, S. G. Lucas, J. A. Spilmann, M. G. Lockley, A. R. C. Milner, & J. I. Kirkland (Eds.), *The Triassic-Jurassic terrestrial transition* (Vol. 37, pp. 548–562). New Mexico Museum of Natural History and Science Bulletin.

Jones, M. E. H. (2008). Skull shape and feeding strategy in *Sphenodon* and other Rhynchocephalia (Diapsida: Lepidosauria). *Journal of Morphology*, *269*, 945–966.

Jones, M. E. H., Anderson, C. L., Hipsley, C. A., Müller, J., Evans, S. E., & Schoch, R. R. (2013). Integration of molecules and new fossils supports a Triassic origin for Lepidosauria (lizards, snakes, and tuatara). *BMC Evolutionary Biology*, *13*, 1–21.

Jones, M. E. H., & Cree, A. (2012). Tuatara. *Current Biology*, *22*(23), R986–R987.

Jones, M. E. H., Curtis, N., O'Higgins, P., Fagan, M., & Evans, S. E. (2009). The head and neck muscles associated with feeding in *Sphenodon* (Reptilia: Lepidosauria: Rhynchocephalia). *Palaeontologia Electronica*, *12*(2), 1–56.

Jones, M. E. H., Tennyson, A. J., Worthy, J. P., Evans, S. E., & Worthy, T. H. (2009). A sphenodontine (Rhynchocephalia) from the Miocene of New Zealand and palaeobiogeography of the tuatara (Sphenodon). *Royal Society B: Biological Sciences*, *276*(1660), 1385–1390.

Kammerer, C. F., Flynn, J. J., Ranivoharimanana, L., & Wyss, A. R. (2012). Ontogeny in the Malagasy traversodontid *Dadadon isaloi* and a reconsideration of its phylogenetic relationships. *Fieldiana Life and Earth Sciences*, *5*, 112–125.

Keeble, E., Whiteside, D. I., & Benton, M. J. (2018). The terrestrial fauna of the Late Triassic Pant-y-ffynnon Quarry fissures, South Wales, UK and a new species of Clevosaurus (Lepidosauria: Rhynchocephalia). *Proceedings of the Geologists Association*, *129*(2), 99–119.

Kim, R., & Evans, D. (2014). Relationships among brain, Endocranial cavity, and body sizes in reptiles. In: Society of Vertebrate Paleontology, 74th Annual Meeting, p. 159.

Klein, C. G., Whiteside, D. I., de Lucas, V. S., Viegas, P. A., & Benton, M. J. (2015). A distinctive Late Triassic microvertebrate

fissure fauna and a new species of Clevosaurus (Lepidosauria: Rhynchocephalia) from Woodleaze Quarry, Gloucestershire, UK. *Proceedings of the Geologists Association*, *126*(3), 402–416.

Köhler, M., Moyá-Solà, S., & Esteban-Trivigno, S. (2008). Morphological variables and associated individual body weight for bovids; new equations for body mass predictions. *Mitteilungen aus dem Hamburgischen Zoologischen Museum und Institut*, *105*, 103–136.

Kotrschal, K., Van Staaden, M. J., & Huber, R. (1998). Fish brains: Evolution and environmental relationships. *Reviews in Fish Biology and Fisheries*, *8*(4), 373–408.

Lamar, S. K., Nelson, N. J., Moore, J. A., Taylor, H. R., Keall, S. N., & Ormsby, D. K. (2021). Initial collection, characterization, and storage of tuatara (*Sphenodon punctatus*) sperm offers insight into their unique reproductive system. *PLoS One*, *16*(7), e0253628.

Langer, M. C., Ramezani, J., & Da Rosa, Á. A. (2018). U-Pb age constraints on dinosaur rise from South Brazil. *Gondwana Research*, *57*, 133–140.

Lautenschlager, S., & Butler, R. J. (2016). Neural and endocranial anatomy of Triassic phytosaurian reptiles and convergence with fossil and modern crocodylians. *PeerJ*, *4*, e2251.

Lautenschlager, S., Ferreira, G. S., & Werneburg, I. (2018). Sensory evolution and ecology of early turtles revealed by digital endocranial reconstructions. *Frontiers in Ecology and Evolution*, *6*, 1–16.

Lautenschlager, S., & Hübner, T. (2013). Ontogenetic trajectories in the ornithischian endocranium. *Journal of Evolutionary Biology*, *26*(9), 2044–2050.

Lefebvre, L., Reader, S. M., & Sol, D. (2004). Brains, innovations and evolution in birds and primates. *Brain, Behavior and Evolution*, *63*, 233–246.

Lessner, E. J., & Holliday, C. M. (2020). A 3D ontogenetic atlas of *Alligator mississippiensis* cranial nerves and their significance for comparative neurology of reptiles. *The Anatomical Record*, *305*(10), 1–29.

Macrì, S., Savriama, Y., Khan, I., & Di-Poï, N. (2019). Comparative analysis of squamate brains unveils multi-level variation in cerebellar architecture associated with locomotor specialization. *Nature Communications*, *10*(1), 1–16.

Macrini, T. E., Rowe, T., & VandeBerg, J. L. (2007). Cranial endocasts from a growth series of *Monodelphis domestica* (Didelphidae, Marsupialia): A study of individual and ontogenetic variation. *Journal of Morphology*, *268*(10), 844–865.

Maisano, J. (2001a). "Sphenodon punctatus" (On-line). Digital Morphology. http://digimorph.org/specimens/Sphenodon_punctatus/juvenile/

Maisano, J. (2001b). "Sphenodon punctatus" (On-line). Digital Morphology. http://digimorph.org/specimens/Sphenodon_punctatus/adult/

Manley, G. A. (1972). A review of some current concepts of the functional evolution of the ear in terrestrial vertebrates. *Evolution*, *26*(4), 608–621.

Marino, L. (2002). Convergence of complex cognitive abilities in cetaceans and primates. *Brain, Behavior and Evolution*, *59*(1–2), 21–32.

Martínez, R. N., Apaldetti, C., Colombi, C. E., Praderio, A., Fernandez, E., Malnis, P. S., Correa, G. A., Abelin, D., & Alcober, O. (2013). A new sphenodontian (Lepidosauria: Rhynchocephalia) from the Late Triassic of Argentina and early origin of herbivore ophistodontians. *Proceedings of the Royal Society B*, *280*, 20132057.

McNamara, K. J. (2012). Heterochrony: The evolution of development. *Evolution: Education and Outreach*, *5*(2), 203–218.

Meloro, C., & Jones, M. E. H. (2012). Tooth and cranial disparity in the fossil relatives of *Sphenodon* (Rhynchocephalia) dispute the persistent 'living fossil' label. *Journal of Evolutionary Biology*, *25*, 2194–2209.

Northcutt, R. G. (2002). Understanding vertebrate brain evolution. *Integrative and Comparative Biology*, *42*, 743–756.

Northcutt, R. G. (2013). Variation in reptilian brains and cognition. *Brain, Behavior and Evolution*, *82*(1), 45–54.

Northcutt, R. G., & Heath, J. E. (1973). T-maze behavior of the tuatara (*Sphenodon punctatus*). *Copeia*, *1973*(3), 617–620.

Ocampo, D., Barrantes, G., & Uy, J. A. C. (2018). Morphological adaptations for relatively larger brains in hummingbird skulls. *Ecology and Evolution*, *8*(21), 10482–10488.

Olori, J. C. (2010). Digital endocasts of the cranial cavity and osseous labyrinth of the burrowing snake *Uropeltis woodmasoni* (Alethinophidia: Uropeltidae). *Copeia*, *1*, 14–26.

Palci, A., Hutchinson, M. N., Caldwell, M. W., & Lee, M. S. Y. (2017). The morphology of the inner ear of squamate reptiles and its bearing on the origin of snakes. *Royal Society Open Science*, *4*, 170685.

Paulina-Carabajal, A. (2017). Secretos guardados en la cabeza de animales extintos. *Desde la patagonia difundiendo saberes*, *14*(23), 14–21.

Paulina-Carabajal, A., & Canale, J. I. (2010). Cranial endocast of the carcharodontosaurid theropod *Giganotosaurus carolinii* Coria & Salgado, 1995. *Neues Jahrbuch für Geologie und Paläontologie - Abhandlungen*, *258*, 249–256.

Paulina-Carabajal, A., Jiménez-Huidobro, P., Triviño, L. N., Stanley, E. L., Zaher, H., & Daza, J. D. (2022). A look in to the Neurocranium of living and extinct Lepidosauria. In M. T. Dozo, A. Paulina-Carabajal, T. E. Macrini, & S. Walsh (Eds.), *Paleoneurology of amniotes* (pp. 123–177). Springer.

Perez-Martinez, C. A., & Leal, M. (2021). Lizards as models to explore the ecological and neuroanatomical correlates of miniaturization. *Behaviour*, *158*(12–13), 1121–1168.

Platel, R. (1989). Anatomy of the brain of the New Zealand gray *Sphenodon punctatus* (Sphenodontidae): A quantitative study of the principle subdivisions of the brain. *Journal für Hirnforschung*, *30*, 325–337.

Rauhut, O. W. M., Heyng, A. M., López-Arbarello, A., & Hecker, A. (2012). A new rhynchocephalian from the Late Jurassic of Germany with a dentition that is unique amongst tetrapods. *PLoS One*, *7*, 46839.

Reiner, A., & Northcutt, R. G. (2000). Succinic dehydrogenase histochemistry reveals the location of the putative primary visual and auditory areas within the dorsal ventricular ridge of Sphenodon punctatus. *Brain, Behavior and Evolution*, *55*(1), 26–36.

Reynoso, V. H. (2000). An unusual aquatic sphenodontian (Reptilia: Diapsida) from the Tlayua Formation (Albian), Central Mexico. *Journal of Paleontology*, *74*(1), 133–148.

Rieppel, O. (1992). The skull in a hatchling of *Sphenodon punctatus*. *Journal of Herpetology*, *26*(1), 80–84.

Robb, J. (1977). *The tuatara*. Meadowfield Press.

Robinson, P. L. (1976). How *Sphenodon* and *Uromastyx* grow their teeth and use them. In A.d.' A. Bellairs & C. B. Cox

(Eds.), *Morphology and biology of reptiles* (pp. 43–64). Academic Press.

Roese-Miron, L., Jones, M., Ferreira, J., & Hsiou, A. (2023). 3D models related to the publication: Virtual endocasts of *Clevosaurus brasiliensis* and the tuatara: Rhynchocephalian neuroanatomy and the oldest endocranial record for Lepidosauria. *MorphoMuseuM*, *8*, e185. https://doi.org/10.18563/journal.m3.185

Romo-de-Vivar, P. R., Martinelli, A. G., Hsiou, A. S., & Soares, M. B. (2020). A new rhynchocephalian from the Late Triassic of southern Brazil enhances Eusphenodontian diversity. *Journal of Systematic Palaeontology*, *18*(13), 1103–1126.

Säilä, L. K. (2005). A new species of the sphenodontian reptile *Clevosaurus* from the lower Jurassic of South Wales. *Palaeontology*, *48*, 817–831.

Sakai, S. T., Arsznov, B. M., Lundrigan, B. L., & Holekamp, K. E. (2011). (b). Brain size and social complexity: A computed tomography study in hyaenidae. *Brain, Behavior and Evolution*, *77*(2), 91–104.

Scanferla, A. (2022). A glimpse into the evolution of the ophidian brain. In D. Gower & H. Zaher (Eds.), *The origin and Early evolutionary history of snakes* (pp. 294–315). Cambridge University Press.

Schade, M., Stumpf, S., Kriwet, J., Kettler, C., & Pfaff, C. (2022). Neuroanatomy of the nodosaurid *Struthiosaurus austriacus* (Dinosauria: Thyreophora) supports potential ecological differentiations within Ankylosauria. *Scientific Reports*, *12*(1), 144.

Scharf, I., Feldman, A., Novosolov, M., Pincheira-Donoso, D., Das, I., Böhm, M., Uetz, P., Torres-Carvajal, O., Bauer, A., Roll, U., & Meiri, S. (2015). Late bloomers and baby boomers: Ecological drivers of longevity in squamates and the tuatara. *Global Ecology and Biogeography*, *24*(4), 396–405.

Schoch, R. R., & Sues, H. D. (2018). A new lepidosauromorph reptile from the Middle Triassic (Ladinian) of Germany and its phylogenetic relationships. *Journal of Vertebrate Paleontology*, *38*(2), e1444619.

Schultz, C. L., Scherer, C. D. S., & Barberena, M. C. (2000). Biostratigraphy of southern Brazilian middle-upper Triassic. *Revista Brasileira de Geociencias*, *30*(3), 491–494.

Schwab, I. R., & O'Connor, G. R. (2005). The lonely eye. *The British Journal of Ophthalmology*, *89*(3), 256.

Segall, M., Cornette, R., Rasmussen, A. R., & Raxworthy, C. J. (2021). Inside the head of snakes: Influence of size, phylogeny, and sensory ecology on endocranium morphology. *Brain Structure & Function*, *226*(7), 2401–2415.

Simões, T. R., Caldwell, M. W., & Pierce, S. E. (2020). Sphenodontian phylogeny and the impact of model choice in Bayesian morphological clock estimates of divergence times and evolutionary rates. *BMC Biology*, *18*(1), 1–30.

Simões, T. R., Kinney-Broderick, G., & Pierce, S. E. (2022). An exceptionally preserved *Sphenodon*-like sphenodontian reveals deep time conservation of the tuatara skeleton and ontogeny. *Communications Biology*, *5*(1), 195.

Smaers, J. B., & Soligo, C. (2013). Brain reorganization, not relative brain size, primarily characterizes anthropoid brain evolution. *Proceedings of the Royal Society B: Biological Sciences*, *280*, 20130269.

Soares, M. B., Schultz, C. L., & Horn, B. L. (2011). New information on *Riograndia guaibensis* Bonaparte, Ferigolo and Ribeiro, 2001 (Eucynodontia, Tritheledontidae) from the Late Triassic of southern Brazil: Anatomical and biostratigraphic implications. *Anais da Academia Brasileira de Ciências*, *83*(1), 329–354.

Starck, D. (1979). Cranio-cerebral relations in recent reptiles. In A. C. Gans, R. G. Northcutt, & P. Ulinski (Eds.), *Biology of the Reptilia* (Vol. 9, pp. 1–36). Academic Press.

Striedter, G. F. (2005). *Principles of brain evolution* (1st ed.). Sinauer.

Sues, H.-D., & Reisz, R. (1995). First record of the early Mesozoic sphenodontian Clevosaurus (Lepidosauria: Rhynchocephalia) from the southern hemisphere. *Journal of Paleontology*, *69*(1), 123–126.

Sues, H. D., Shubin, N. H., & Olsen, P. E. (1994). A new sphenodontian (Lepidosauria: Rhynchocephalia) from the McCoy Brook Formation (Lower Jurassic) of Nova Scotia, Canada. *Journal of Vertebrate Paleontology*, *14*, 327–340.

Thompson, M. B., & Daugherty, C. H. (1998). Metabolism of tuatara, *Sphenodon punctatus*. *Comparative Biochemistry and Physiology. Part A, Molecular & Integrative Physiology*, *119*(2), 519–522.

Triviño, L. N., Albino, A. M., Dozo, M. T., & Williams, J. D. (2018). First natural endocranial cast of a fossil snake (Cretaceous of Patagonia, Argentina). *The Anatomical Record*, *301*, 9–20.

van Schaik, C. P., Triki, Z., Bshary, R., & Heldstab, S. A. (2021). A farewell to the encephalization quotient: A new brain size measure for comparative primate cognition. *Brain, Behavior and Evolution*, *96*(1), 1–12.

Vaux, F., Morgan-Richards, M., Daly, E. E., & Trewick, S. A. (2018). Tuatara and a new morphometric dataset for Rhynchocephalia: Comments on Herrera-Flores et al. *Palaeontology*, *62*(2), 321–334.

Vickerton, P., Jarvis, J., & Jeffery, N. (2013). Concentration-dependent specimen shrinkage in iodine-enhanced micro CT. *Journal of Anatomy*, *223*(2), 185–193.

Walsh, S. A., Barrett, P. M., Milner, A. C., Manley, G., & Witmer, L. M. (2009). Inner ear anatomy is a proxy for deducing auditory capability and behaviour in reptiles and birds. *Proceedings of the Royal Society B: Biological Sciences*, *276*(1660), 1355–1360.

Walsh, S. A., & Knoll, M. A. (2011). Directions in palaeoneurology. *Palaeontology*, *86*, 263–279.

Watanabe, A., Gignac, P. M., Balanoff, A. M., Green, T. L., Kley, N. J., & Norell, M. A. (2019). Are endocasts good proxies for brain size and shape in archosaurs throughout ontogeny? *Journal of Anatomy*, *234*(3), 291–305.

Whiteside, D. I. (1986). The head skeleton of the Rhaetian sphenodontid *Diphydontosaurus avonis* gen. et sp. nov. and the modernizing of a living fossil. *Philosophical Transactions of the Royal Society B: Biological Sciences*, *312*(1156), 379–430.

Witmer, L. M., Chatterjee, S., Franzosa, J., & Rowe, T. (2003). Neuroanatomy of flying reptiles and implications for flight, posture and behaviour. *Nature*, *425*(6961), 950–953.

Wu, X.-C. (1994). Late Triassic-Early Jurassic sphenodontians from China and the phylogeny of the Sphenodontia. In N. C. Fraser & H. D. Sues (Eds.), *In the shadow of the dinosaurs* (pp. 38–69). Cambridge University Press.

Wu, X.-C. (2003). Functional morphology of the temporal region in the Rhynchocephalia. *Canadian Journal of Earth Sciences*, *40*(4), 589–607.

Wyeth, F. J. (1920). On the development of the auditory apparatus in *Sphenodon punctatus*. *Proceedings of the Royal Society of London. Series B, Biological Sciences*, *91*(639), 224–228.

Yi, H., & Norell, M. (2019). The bony labyrinth of *Platecarpus* (Squamata: Mosasauria) and aquatic adaptations in squamate reptiles. *Palaeoworld*, *28*(4), 550–561.

Yi, H., & Norell, M. A. (2015). The burrowing origin of modern snakes. *Science Advances*, *1*(10), e1500743.

Zerfass, H., Lavina, E. L., Schultz, C. L., Garcia, A. J. V., Faccini, U. F., & Chemale, F., Jr. (2003). Sequence stratigraphy of continental Triassic strata of Southernmost Brazil: A contribution to Southwestern Gondwana palaeogeography and palaeoclimate. *Sedimentary Geology*, *161*(1–2), 85–105.

SUPPORTING INFORMATION

Additional supporting information can be found online in the Supporting Information section at the end of this article.

How to cite this article: Roese-Miron, L., Jones, M. E. H., Ferreira, J. D., & Hsiou, A. S. (2023). Virtual endocasts of *Clevosaurus brasiliensis* and the tuatara: Rhynchocephalian neuroanatomy and the oldest endocranial record for Lepidosauria. *The Anatomical Record*, 1–24. https://doi.org/10.1002/ar.25212